

**Winter CO<sub>2</sub> emission  
in Paris**

M. Lopez et al.

# Isotope- and tracer-based measurements of fossil fuel and biospheric carbon dioxide in Paris during winter 2010

M. Lopez<sup>1</sup>, M. Schmidt<sup>1</sup>, M. Delmotte<sup>1</sup>, A. Colomb<sup>2,\*</sup>, V. Gros<sup>1</sup>, C. Janssen<sup>3</sup>, S. J. Lehman<sup>4</sup>, D. Mondelain<sup>3,\*\*</sup>, O. Perrussel<sup>5</sup>, M. Ramonet<sup>1</sup>, I. Xueref-Remy<sup>1</sup>, and P. Bousquet<sup>1</sup>

<sup>1</sup>Laboratoire des Sciences du Climat et de l'Environnement (LSCE), Unité mixte CEA-CNRS-UVSQ, UMR8212, 91191 Gif-sur-Yvette, France

<sup>2</sup>Laboratoire Interuniversitaire des Systèmes Atmosphériques (LISA), CNRS-IPSL, 94010 Creteil, France

<sup>3</sup>Laboratoire de Physique Moléculaire pour l'Atmosphère et l'Astrophysique (LPMAA), CNRS, Université Pierre et Marie Curie, 75005 Paris, France

<sup>4</sup>Institute of Arctic and Alpine Research (INSTAAR), University of Colorado, Boulder, USA

<sup>5</sup>AIRPARIF, Association de Surveillance de la Qualité de l'Air en Ile-de-France, Paris, France

\* now at: Laboratoire de Métrologie Physique (LaMP), CNRS, 63171 Aubière, France

\*\* now at: Laboratoire Interdisciplinaire de Physique (LiPhy), CNRS, Université Joseph Fourier, 38402 Saint Martin d'Hères, France

Title Page

Abstract

Introduction

Conclusions

References

Tables

Figures

◀

▶

◀

▶

Back

Close

Full Screen / Esc

Printer-friendly Version

Interactive Discussion



Received: 19 December 2012 – Accepted: 2 January 2013 – Published: 22 January 2013

Correspondence to: M. Lopez (morgan.lopez@lsce.ipsl.fr)

Published by Copernicus Publications on behalf of the European Geosciences Union.

ACPD

13, 2371–2414, 2013

## Winter CO<sub>2</sub> emission in Paris

M. Lopez et al.

Title Page

Abstract

Introduction

Conclusions

References

Tables

Figures



Back

Close

Full Screen / Esc

Printer-friendly Version

Interactive Discussion



## Abstract

Measurements of the mole fraction of the CO<sub>2</sub> and its isotopes were performed in Paris during the MEGAPOLI winter campaign (January–February 2010). Radiocarbon (<sup>14</sup>CO<sub>2</sub>) measurements were used to identify the relative contributions of 77 % CO<sub>2</sub> from fossil fuel consumption (CO<sub>2</sub>ff from liquid and gas combustion) and 23 % from biospheric CO<sub>2</sub> (CO<sub>2</sub> from the use of biofuels and from human and plant respiration: CO<sub>2</sub>bio). These percentages correspond to average mole fractions of 26.4 ppm and 8.2 ppm for CO<sub>2</sub>ff and CO<sub>2</sub>bio, respectively. The <sup>13</sup>CO<sub>2</sub> analysis indicated that gas and liquid fuel contributed 70 % and 30 %, respectively, of the CO<sub>2</sub> emission from fossil fuel use. Continuous measurements of CO and NO<sub>x</sub> and the ratios  $\frac{\text{CO}}{\text{CO}_{2\text{ff}}}$  and  $\frac{\text{NO}_x}{\text{CO}_{2\text{ff}}}$  derived from radiocarbon measurements during four days make it possible to estimate the fossil fuel CO<sub>2</sub> contribution over the entire campaign. The ratios  $\frac{\text{CO}}{\text{CO}_{2\text{ff}}}$  and  $\frac{\text{NO}_x}{\text{CO}_{2\text{ff}}}$  are functions of air mass origin and exhibited daily ranges of 7.9 to 14.5 ppb ppm<sup>-1</sup> and 1.1 to 4.3 ppb ppm<sup>-1</sup>, respectively. These ratios are sufficiently consistent with different emission inventories given the uncertainties of the different approaches.

## 1 Introduction

Worldwide, approximately 20 “megacities” have a population of more than 10 million inhabitants. According to the United Nations, half of the world’s population now lives in cities, and in the near future, the number of megacities and their population density figures are expected to grow considerably. In the context of global warming and in the framework of the Kyoto Protocol, it is important to better characterise greenhouse gas (GHG) emissions from megacities, which constitute a significant emission source at the global scale. More than 70 % of global fossil-fuel CO<sub>2</sub> emissions are concentrated in cities (Duren and Miller, 2012).

ACPD

13, 2371–2414, 2013

## Winter CO<sub>2</sub> emission in Paris

M. Lopez et al.

Title Page

Abstract

Introduction

Conclusions

References

Tables

Figures

◀

▶

◀

▶

Back

Close

Full Screen / Esc

Printer-friendly Version

Interactive Discussion



## Winter CO<sub>2</sub> emission in Paris

M. Lopez et al.

Title Page

Abstract

Introduction

Conclusions

References

Tables

Figures

◀

▶

◀

▶

Back

Close

Full Screen / Esc

Printer-friendly Version

Interactive Discussion



With 12 million inhabitants (approximately 18 % of the French population), Paris and its suburbs constitute the largest megacity in Europe. According to the regional French emission inventory provided by AirParif (<http://www.airparif.asso.fr/>), CO<sub>2</sub> emissions from Paris and its agglomeration (the Ile-de-France region or IdF) were 50 Mt in 2005, or 13 % of the total French anthropogenic CO<sub>2</sub> emissions, although the IdF region, with a surface area of 12 011 km<sup>2</sup>, composes only 1.8 % of the French territory. The annual CO<sub>2</sub> emission density within the IdF region increases from approximately 5000 t CO<sub>2</sub> km<sup>-2</sup> at the border of the suburbs to approximately 70 000 t CO<sub>2</sub> km<sup>-2</sup> at the centre of Paris, reflecting the change in population density. Based on the Kyoto Protocol, France is committed to reducing its greenhouse gas emissions by 8 % with respect to its 1990 emissions by 2012. A decrease of 6.0 % was observed in 2010 compared to the reference year 1990, primarily due to reductions in N<sub>2</sub>O and CO<sub>2</sub> emissions (CITEPA, 2012). In addition, France adopted the “climate and energy package”, which aims to reduce greenhouse gas emissions by 20 % with respect to 2005 emissions by 2020.

Currently, regional and local GHG emissions data are primarily derived from statistical inventories that are gathered using a bottom-up method that involves the compilation of activity and process data. Economic statistics are gathered from the local to the national level to produce gridded maps of GHG emissions (EDGAR: Olivier et al., 2001; Olivier and Berdowsky, 2001). Peylin et al. (2011) showed that such emission inventories can vary up to 40 % on the national scale even for developed countries like the Netherlands, where we can expect the best datasets available for use in compiling the inventory. Atmospheric measurements can provide an alternative to develop methods of emission verification, in association with bottom-up inventories. Atmospheric methods (top-down methods) rely on a combination of high precision measurements of atmospheric mole fractions of GHGs such as CO<sub>2</sub> and on measurements of atmospheric tracers and atmospheric transport models. At global to regional scales, inverse models have been used successfully to quantify GHG emissions for CO<sub>2</sub> (Rayner and Law, 1999; Bousquet et al., 2000; Rödenbeck et al., 2003; Peylin et al., 2005), CH<sub>4</sub>

(Rödenbeck, 2005; Bousquet et al., 2006), and N<sub>2</sub>O (Hirsch et al., 2006; Thompson et al., 2011). On the local and regional scales, continuous observations of GHGs can be combined with observations of radon-222, which is used as a tracer for atmospheric dilution (van der Laan et al., 2009; Yver et al., 2009; Hammer and Levin, 2009) to estimate surface emissions.

The use of atmospheric measurements of CO<sub>2</sub> to estimate surface emissions in urban areas is of growing interest. During the last several years, a few projects focused on quantifying CO<sub>2</sub> fluxes from cities using top-down approaches emerged in the USA and in France, including the InFLUX project in Indianapolis, USA (<http://influx.psu.edu/>), the Los Angeles Megacity project (Duren and Miller, 2012), and the CO<sub>2</sub>-Megaparis project in Paris (<https://co2-megaparis.lsce.ipsl.fr>). One challenging issue associated with atmospheric top-down approach is the attribution of emissions to specific processes. The first step in this process is to distinguish between CO<sub>2</sub> emitted from anthropogenic activities and CO<sub>2</sub> emitted from biospheric activities. Even in urban areas, variations in the atmospheric CO<sub>2</sub> mole fraction contain signatures from both fossil fuel combustion and biogenic sources. These signatures can be decrypted by additional information that is provided by specific tracers. Only <sup>14</sup>CO<sub>2</sub> measurements allow for the direct quantification of the contribution of fossil fuel CO<sub>2</sub> to observed CO<sub>2</sub> mole fractions (Levin et al., 2003; Turnbull et al., 2006; Vogel et al., 2010) because CO<sub>2</sub> from fossil fuels does not contain <sup>14</sup>C. Levin and Karstens (2007) showed that fossil fuel emissions and biospheric fluxes are of similar orders of magnitude in Europe. Because precise <sup>14</sup>CO<sub>2</sub> measurements are difficult to perform, carbon monoxide is often used as a tracer for fossil fuel CO<sub>2</sub> emissions (CO<sub>2</sub>ff), to separate the biospheric and the fossil fuel components from the total measured CO<sub>2</sub> mole fraction. The CO/CO<sub>2</sub>ff ratio depends on the condition of combustion and on the fuel type and can range from 17.5 ppb CO ppm<sup>-1</sup> CO<sub>2</sub> for industrial sources and 14.5 ppb CO ppm<sup>-1</sup> CO<sub>2</sub> for residential heating to 5.3 ppb CO ppm<sup>-1</sup> CO<sub>2</sub> for traffic according to the national emission inventories by the Centre Interprofessionnel Technique d'Etude de la Pollution Atmospherique (CITEPA, <http://www.citepa.org/>) for the year

**Winter CO<sub>2</sub> emission  
in Paris**

M. Lopez et al.

Title Page

Abstract

Introduction

Conclusions

References

Tables

Figures

◀

▶

◀

▶

Back

Close

Full Screen / Esc

Printer-friendly Version

Interactive Discussion



2010 in France. From 2000 to 2010, improvements in combustion efficiency due to regulations that are attended to improve air quality led to a significant reduction in CO emissions and also to changes in CO/CO<sub>2</sub> fossil fuel ratios, which decreased from 20 to 13 ppb CO ppm<sup>-1</sup> CO<sub>2</sub> in France. This reduction was primarily caused by the introduction of catalytic converters for cars, which decreased of the road traffic CO/CO<sub>2</sub> ratio from 21 to 5 ppb CO ppm<sup>-1</sup> CO<sub>2</sub>.

The European project MEGAPOLI (Megacities: Emissions, urban, regional and Global Atmospheric POLLution and climate effects, and Integrated tools for assessment and mitigation, <http://www.megapoli.info>) aims to assess the impact of megacities on air pollution, to quantify the feedback regarding megacity air quality, and to develop integrated tools for predicting air pollution in megacities. To address these three objectives, the MEGAPOLI project organised two intensive measurement campaigns in Paris: one in July 2009 and one in January–February 2010. During the campaigns, numerous atmospheric pollutants and parameters were monitored by different groups (Royer et al., 2011; Healy et al., 2012; Dolgorouky et al., 2012). The French Atmospheric Network for Greenhouse Gases Monitoring (RAMCES), which is part of the Laboratory for Climate and Environmental Sciences (LSCE), participated in the frame of the CO<sub>2</sub>-Megaparis project to the measurement campaign in the winter of 2010, which extended from 15 January to 19 February. During this campaign, we focused on continuous CO<sub>2</sub> and CO measurement in Paris and the Plateau of Saclay (20 km south-west of Paris, Sect. 2). In addition, air was sampled in flasks for <sup>14</sup>CO<sub>2</sub> analysis (Sect. 3.1). Radiocarbon and stable CO<sub>2</sub> isotope measurements were used to compute the respective contributions of fossil fuels and biospheric CO<sub>2</sub> to the overall CO<sub>2</sub> mole fraction in Paris (Sects. 3.2 and 3.3). These direct estimations of CO<sub>2</sub> were used to evaluate the potential of alternative proxies to radiocarbon such as CO and NO<sub>x</sub> (Sect. 3.4).

**Winter CO<sub>2</sub> emission  
in Paris**

M. Lopez et al.

Title Page

Abstract

Introduction

Conclusions

References

Tables

Figures

◀

▶

◀

▶

Back

Close

Full Screen / Esc

Printer-friendly Version

Interactive Discussion



## 2 Methods

### 2.1 Description of measurement stations

#### 2.1.1 Paris

Paris is the largest city in France; it has 2.2 million inhabitants (source: INSEE, January 2009) and a population density of 21 196 inhabitants per square kilometre which is one of the highest densities in Europe. Paris and its suburbs include several industrial and transportation hot spots, although numerous polluting industrial activities were removed from the Paris agglomeration in the 1960s. Two sites were instrumented for atmospheric measurements within the city centre during the MEGAPOLI campaign. The Laboratoire de l'Hygiène de la Ville de Paris (LHVP), located at 48°50' N, 2°21' E and at 62 m above sea level (a.s.l.), lies within the southern part of Paris (13th district). This laboratory is located on the edge of the Parc de Choisy, approximately 100 m from a main road. A large number of instruments were deployed at the LHVP station to monitor atmospheric compounds such as aerosols, volatile organic compounds (VOCs), ozone, nitrogen oxides ( $\text{NO}_x = \text{NO} + \text{NO}_2$ ), and meteorological parameters. A cavity ring down spectrometer (CRDS) was installed for continuous atmospheric carbon dioxide ( $\text{CO}_2$ ) and carbon monoxide (CO) measurement, and a flask sampling unit was also installed. All inlet lines were positioned on the roof of the LHVP, 15 m above the ground level (agl) in a vented location.

A second site was equipped for atmospheric measurements at the QualAir station in Jussieu (<http://qualair.aero.jussieu.fr/>), a campus of University Pierre et Marie Curie, 48°51' N, 2°21' E and 38 m a.s.l., which is located in the city centre of Paris. This station is approximately 2 km from the LHVP. This site was already equipped with several atmospheric monitoring instruments (including those for CO measurement) and was adapted to use larger instruments than those at the LHVP. An automatic flask sampler (Neubert et al., 2004) and a tunable diode laser (TDL) spectrometer, developed and operated by the Laboratory of Molecular Physics for Atmosphere and Astrophysics

## Winter $\text{CO}_2$ emission in Paris

M. Lopez et al.

Title Page

Abstract

Introduction

Conclusions

References

Tables

Figures

◀

▶

◀

▶

Back

Close

Full Screen / Esc

Printer-friendly Version

Interactive Discussion



(LPMAA, Croizé et al., 2010), were installed for continuous CO<sub>2</sub> and δ<sup>13</sup>CO<sub>2</sub> measurements. The two inlet lines were located on the roof of the building, 22 m a.g.l.

We used the meteorological parameters of the QualAir station (wind speed and wind direction), as these figures are higher for this station because the location is less in the wind shadow of other buildings and therefore is more representative than the LHVP station. During the campaign, wind directions with approximately equal frequency from all four directions and a mean wind speed of 2.7 m s<sup>-1</sup> have been observed.

### 2.1.2 The Plateau of Saclay

The Plateau of Saclay is a semi-urban flat area that is located approximately 20 km south-west of Paris. The Plateau contains atmospheric measurement stations at Gif-sur-Yvette and SIRTAs, which are 5 km apart. The sites are mainly surrounded by agricultural fields, forests and villages and can be described as sub-urban.

Gif-sur-Yvette station (Gif station), 48°42' N, 02°09' E and 160 m a.s.l., is part of the LSCE and belongs to the RAMCES team. The closest villages and small towns are Saint-Aubin (673 inhabitants) and Gif-sur-Yvette (21 352 inhabitants), which are located 500 m north-west and 1 km south of the station, respectively (Yver et al., 2009). The station is equipped with a gas chromatograph (GC) system that performs continuous measurements of CO<sub>2</sub>, CH<sub>4</sub>, N<sub>2</sub>O, SF<sub>6</sub>, CO and H<sub>2</sub> (Pépin et al., 2001; Yver et al., 2009; Lopez et al., 2012). The analytical laboratory is also equipped with an isotope ratio mass spectrometer (IRMS) that is dedicated to the atmospheric measurement of CO<sub>2</sub> isotopes: δ<sup>13</sup>C and δ<sup>18</sup>O (WMO-GAW, 2005). The inlet lines are located on the roof of the laboratory building, 7 m a.g.l.

The Instrumental Site of Research by Atmospheric Remote Sensing observatory (SIRTA, Haeffelin et al., 2005), located at 48°43' N, 02°12' E and 156 m a.s.l., in Palaiseau, is approximately 4.5 km east of Gif-sur-Yvette station. During the winter campaign, NO<sub>x</sub> was monitored by the Interuniversity Laboratory of Atmospheric Systems (LISA).

## Winter CO<sub>2</sub> emission in Paris

M. Lopez et al.

Title Page

Abstract

Introduction

Conclusions

References

Tables

Figures

◀

▶

◀

▶

Back

Close

Full Screen / Esc

Printer-friendly Version

Interactive Discussion



**Winter CO<sub>2</sub> emission  
in Paris**

M. Lopez et al.

Title Page

Abstract

Introduction

Conclusions

References

Tables

Figures

◀

▶

◀

▶

Back

Close

Full Screen / Esc

Printer-friendly Version

Interactive Discussion



During the 2010 winter campaign, two primary wind regimes were observed: winds from the north ( $0^{\circ}$ – $45^{\circ}$ ) that blew 22 % of the time and transported polluted air masses from Paris and winds from the west ( $225^{\circ}$ – $270^{\circ}$  wind sector) that also blew 22 % of the time. The mean wind speed in both cases was  $5.4 \text{ m s}^{-1}$ . During the rest of time, the wind regimes were well distributed among the remaining sectors except for the eastern one ( $45^{\circ}$ – $90^{\circ}$ ), which was under-represented (with winds blowing from that direction less than 3 % of time).

### 2.1.3 Trainou station

Trainou station ( $47^{\circ}57' \text{ N}$ ,  $02^{\circ}06' \text{ E}$ , 131 m a.s.l.) is a site located 100 km south of Paris that is mainly surrounded by agricultural fields and forests. The nearest city is Orléans, which is 15 km south-west of the site and has 116 000 inhabitants. Trainou can thus be considered a rural site, especially in comparison to the Paris area. Air inlet lines are located at 5, 50, 100 and 180 m a.g.l. on a television tower (TeleDiffusion de France). Continuous GC analysis for  $\text{CO}_2$ ,  $\text{CH}_4$ ,  $\text{N}_2\text{O}$ ,  $\text{SF}_6$ ,  $\text{CO}$  and  $\text{H}_2$  mole fractions have been conducted since 2007 (Messenger, 2007; Yver et al., 2010; Lopez et al., 2012). The analysed meteorological variables from the data assimilation system of the European Centre for Medium-Range Weather Forecasts (ECMWF) were used for Trainou station. During the campaign, the station experienced approximately the same wind regimes as Gif-sur-Yvette station, with 24 % of the wind coming from the north-northeast ( $0^{\circ}$ – $45^{\circ}$ ) and 25 % of the wind from the west-southwest ( $225^{\circ}$ – $270^{\circ}$ ). The mean wind speeds were  $4.6 \text{ m s}^{-1}$  and  $4.3 \text{ m s}^{-1}$  for the two sectors, respectively.

## 2.2 Instrumentation and air sampling strategies

### 2.2.1 In situ analysers

The cavity ring down spectrometer (G1302 Picarro, Wastine et al., 2009) that was installed at the LHVP analyses  $\text{CO}_2$ ,  $\text{CO}$  and water vapour ( $\text{H}_2\text{O}$ ) mole fractions with

**Winter CO<sub>2</sub> emission  
in Paris**

M. Lopez et al.

[Title Page](#)[Abstract](#)[Introduction](#)[Conclusions](#)[References](#)[Tables](#)[Figures](#)[◀](#)[▶](#)[◀](#)[▶](#)[Back](#)[Close](#)[Full Screen / Esc](#)[Printer-friendly Version](#)[Interactive Discussion](#)

5 a sampling frequency of 1 Hz. This instrument was calibrated for CO<sub>2</sub> and CO before and after the campaign with four calibration tanks based on the WMO-X2007 scale. During the campaign, two high-pressure cylinders were analysed for 30 min every 10 h for quality control purposes. One cylinder was used as a working standard to correct for potential temporal drift by the analyser, and the second cylinder was used as a target gas to evaluate repeatability. During the measurement period, a systematic drift in the CO<sub>2</sub> raw data of 0.08 ppm per month was observed, whereas no significant variation in the CO measurements was detected. After drift corrections for the entire campaign, the target gas showed a repeatability level (1 sigma) of 0.03 ppm for the CO<sub>2</sub> measurements and 10.1 ppb for the CO measurements when one-minute averages were used. Because the ambient air was not dried prior to the CRDS analysis, a water vapour correction for CO<sub>2</sub> was used together with a constant correction (–15 ppb) for CO measurements, which was empirically determined during several weeks of testing in our laboratory in Gif-sur-Yvette (Kaiser et al., 2010).

15 At Jussieu, a tunable diode laser spectrometer has been installed and operated by the LPMAA to continuously monitor the atmospheric total CO<sub>2</sub> mole fraction and  $\delta^{13}\text{C}$  for four consecutive days in February (Croizé et al., 2010). The analysis technique is based on the absorbance correlations between a sealed reference cell and the sample cell. More details regarding the instrumental set-up and calibration strategy used are provided in Croizé et al. (2010). All of the reference and calibration cylinders used in this instrument were calibrated at the central laboratory of LSCE by GC and IRMS.

20 The two gas chromatographs (Agilent HP-6890 and HP-6890N) located at Gif-sur-Yvette (semi-urban site) and Trainou (rural site) were optimised for semi-continuous atmospheric measurements. The GC are equipped with two detectors to simultaneously analyse CO<sub>2</sub> and CH<sub>4</sub> with a flame ionisation detector (FID, Messenger, 2007) and N<sub>2</sub>O and SF<sub>6</sub> with an electron capture detector (ECD, Lopez et al., 2012). In 2006 at Gif-sur-Yvette and in 2009 at Trainou, two Peak-Performers (PP1) were coupled to the GC for additional analysis of CO and H<sub>2</sub> using a reduction gas detector (RGD, Yver et al., 2009). In addition to continuous measurements, the GC at Gif-sur-Yvette has

been optimised for flask analysis and tank calibration. All of the GC measurements (continuous, flasks and tanks) were calibrated on the WMO-X2007 scale.

The isotope ratio mass spectrometer (Finnigan MAT 252) located at Gif-sur-Yvette measures the isotopic composition of atmospheric CO<sub>2</sub> ( $\delta^{13}\text{C}$  and  $\delta^{18}\text{O}$  in CO<sub>2</sub>) from flasks (Schmidt et al., 2005). An automated sampling line was set-up according to the “BGC-Airtrap” design as described in Werner et al. (2001) to cryogenically separate CO<sub>2</sub> (along with N<sub>2</sub>O) from the other air constituents. The “airtrap” is coupled to the IRMS inlet system and used to analyse the air sampled in the flasks. During the campaign, the IRMS was used for semi-continuous analysis of the atmospheric CO<sub>2</sub> isotopes at Gif-sur-Yvette during a three-day period. Each analysis sequence consisted of injections of an ambient air standard followed by a target gas and up to 10 flasks, another ambient air standard injected at the end. The carbon dioxide isotopic data are reported in the  $\delta$  notation (Eq. 1);  $R$  is the ratio of the heavy isotope to the light one. The  $\delta^{13}\text{C}$  values are referenced to the V-PDB scale.

$$\delta = \left( \frac{R_{\text{sample}}}{R_{\text{standards}}} - 1 \right) \times 1000 \quad (1)$$

In addition to CO<sub>2</sub> and CO, NO<sub>x</sub> has been monitored at the LHVP and SIRTA stations. NO<sub>x</sub> was measured continuously using two chemiluminescent analysers (AC31M, Environment SA) that were operated by the LSCE at the LHVP and by the LISA at SIRTA. A summary of the instrumentation used for this study during the MEGAPOLI campaign is given in Table 1.

## 2.2.2 Flask sampling strategy

In addition to continuous measurements, flask sampling was carried out to collect dried ambient air at the LHVP and Jussieu stations. At the LHVP, a manual sampler was used to fill 43 pairs of one and two litre glass flasks. The flasks were filled in the morning during the traffic rush hour on six days in February. At Jussieu, 35 2.5 L flasks were regularly filled for two complete days and one night. All flasks were analysed using a GC

## Winter CO<sub>2</sub> emission in Paris

M. Lopez et al.

Title Page

Abstract

Introduction

Conclusions

References

Tables

Figures

◀

▶

◀

▶

Back

Close

Full Screen / Esc

Printer-friendly Version

Interactive Discussion



and IRMS to provide additional trace gas information and to independently determine the quality of the continuous CRD ( $\text{CO}_2$  and  $\text{CO}$ ) and TDL ( $\text{CO}_2$ ,  $^{13}\text{C}$ ) spectrometer measurements. We selected 23 flasks (17 from LHVP and 6 sampled at Jussieu) for high-precision  $^{14}\text{CO}_2$  analysis. Flasks were chosen based on the atmospheric  $\text{CO}_2$  mole fraction, and days with large temporal  $\text{CO}_2$  gradients were favoured.

The samples were prepared at the University of Colorado, Boulder, and measurements were performed via accelerator mass spectrometry (AMS) at the University of California, Irvine, following Turnbull et al. (2007). The radiocarbon values are expressed in  $\Delta$  notation (Stuiver and Polach, 1977).

### 2.2.3 Comparison of continuous measurements with flasks sampling

The flask results were compared with the corresponding two-minute averages from the continuous analysers. At the LHVP, the mean difference between 36 pairs of flasks and the CRDS analyser data was  $-0.03 \pm 3.33$  ppm for  $\text{CO}_2$  and  $-1.9 \pm 31.1$  ppb for  $\text{CO}$ , indicating a good agreement in both cases. The comparison between the flasks and the TDL spectrometer for the  $\text{CO}_2$  mole fraction and  $\delta^{13}\text{C}$  also indicates good agreement, with mean differences between the flasks and with in situ measurements of  $0.07 \pm 2.33$  ppm ( $N = 15$ ) for  $\text{CO}_2$  and  $0.29 \pm 0.20$  ‰ ( $N = 16$ ) for  $\delta^{13}\text{C}$ . The substantial standard deviation is likely related to the strong temporal variability in Paris, which often reaches several ppm for  $\text{CO}_2$  and 10 ppb for  $\text{CO}$  in just a few minutes. The 0.29 ‰ mean difference observed in the  $\delta^{13}\text{C}$  analysis may have been caused by an underestimated correction of the TDL spectrometer measurements. The correction aims to account for the small temperature difference between the atmospheric air and the calibration gas after the atmospheric air has been passed through a cold trap to remove water vapour (Croizé et al., 2010).

The mean mole fraction differences for the  $\text{CO}_2$  and  $\text{CO}$  measurements derived from continuous measurement versus flask sampling are consistent with the WMO-GAW recommendation for background measurements: WMO-GAW (2009). The objective is to maintain a network interoperability level of  $\pm 0.1$  ppm and  $\pm 2$  ppb for  $\text{CO}_2$  and  $\text{CO}$ ,

## Winter $\text{CO}_2$ emission in Paris

M. Lopez et al.

Title Page

Abstract

Introduction

Conclusions

References

Tables

Figures

◀

▶

◀

▶

Back

Close

Full Screen / Esc

Printer-friendly Version

Interactive Discussion



respectively. The  $\delta^{13}\text{C}$  figures do not meet the WMO-GAW recommended maximum difference of  $\pm 0.01\text{‰}$ . The substantial difference is due to instrumental accuracy. However, this difference is not likely to impact the conclusions of this study, which shows that large signals are associated with sampling close to sources in a polluted area.

### 3 Results and discussion

#### 3.1 The observation of $\text{CO}_2$ , $\text{CO}$ and $\text{NO}_x$ in Paris, at the Plateau of Saclay and at Trainou station

In the Paris region,  $\text{CO}_2$  is mainly emitted by anthropogenic sources through the combustion of fossil fuel and biomass (wood and biofuel), although natural sources such as soil respiration also contribute to a degree that remains highly uncertain. Carbon monoxide is often considered a reliable combustion tracer, as it results from fossil fuel and biomass burning and has an atmospheric life-time of approximately two months.  $\text{NO}_x$  is a typical marker of traffic exhaust emissions and has a life-time of approximately nine hours (Atkinson et al., 2006). However, due to its short life-time,  $\text{NO}_x$  cannot be transported over long distances and consequently can only be used as a tracer for local emissions.

Figure 1 presents the  $\text{CO}_2$ ,  $\text{CO}$  and  $\text{NO}_x$  mole fractions observed at the LHVP (Paris), at the Plateau of Saclay, and at Trainou tower (TR3, 180 m a.g.l. air inlet) with one-hour time resolution from 15 January 2010 to 19 February 2010. The LHVP yielded the highest  $\text{CO}_2$ ,  $\text{CO}$  and  $\text{NO}_x$  values, and the data exhibit the largest synoptic variability because the station is close to anthropogenic sources. Trainou yielded the lowest values and synoptic variability, which was expected given that we sampled at 180 m a.g.l. and the rural site likely has weaker local  $\text{CO}_2$  and  $\text{CO}$  sources.

The wind regimes were classified based on back trajectories obtained using the Lagrangian particle dispersion model, FLEXPART (version 8.2), which is described by Stohl et al. (2007). In Fig. 1, the yellow areas correspond to times when the air masses

Title Page

Abstract

Introduction

Conclusions

References

Tables

Figures

◀

▶

◀

▶

Back

Close

Full Screen / Esc

Printer-friendly Version

Interactive Discussion



that influenced the sites originated from the western sector (180° to 360°). We refer to this as the “oceanic regime” using the MEGAPOLI project nomenclature. The grey areas correspond to times when air masses came from eastern Europe (0° to 180°) and crossed Germany or Benelux before arriving at the LHVP, the Plateau of Saclay and Trainou station. We refer to this as the “continental regime”. The data collected on days for which air mass back trajectories could not be clearly classified (uncoloured ones) are not considered in the analysis that follows.

Table 2 summarises the average mole fractions of CO<sub>2</sub>, CO and NO<sub>x</sub> for the two different regimes. On average, the three sites show higher CO<sub>2</sub> and CO mole fractions during the continental regime. The average mole fractions for the continental and oceanic regimes are statistically distinct at all three sites with a probability of 98.9% and 99.2% for CO<sub>2</sub> and CO, respectively, at the LHVP and a probability greater than 99.9% for CO<sub>2</sub> and CO at the Plateau of Saclay and Trainou (according to Student's *t*-test). Carbon dioxide and carbon monoxide, with life-times of 120 yr and two months, respectively, can be transported over longer distances than NO<sub>x</sub> can. Thus, higher CO<sub>2</sub> and CO mole fractions are associated with the continental regime because the air masses are progressively charged with pollutants on their trajectory to Paris. When the main wind direction shifts from east (continental) to west (oceanic), a decrease in CO<sub>2</sub> and CO mole fractions is observed. Nitrogen oxides cannot be transported over long distances; thus, at the LHVP and the Plateau of Saclay, NO<sub>x</sub> mole fractions are similar for the oceanic and continental regimes.

Figure 2 shows the mean diurnal cycles of CO<sub>2</sub>, CO and NO<sub>x</sub> at the three stations for both weekdays (in red) and weekends (in black) for the entire measurement period. The mole fractions of trace gases and the mean amplitudes of the diurnal cycles are both smaller, on weekends than on weekdays. The mean CO<sub>2</sub>, CO and NO<sub>x</sub> diurnal cycles show two peaks at LHVP, in the morning (07:00 UTC to 09:00 UTC) and at the end of the afternoon (18:00 UTC to 20:00 UTC). At the Plateau of Saclay, the afternoon peak is weak and is only visible for CO and NO<sub>x</sub>. The mean diurnal cycle of the traffic flow in the IdF region during weekdays for the year 2010 is presented along with the NO<sub>x</sub>

**Winter CO<sub>2</sub> emission  
in Paris**

M. Lopez et al.

[Title Page](#)[Abstract](#)[Introduction](#)[Conclusions](#)[References](#)[Tables](#)[Figures](#)[◀](#)[▶](#)[◀](#)[▶](#)[Back](#)[Close](#)[Full Screen / Esc](#)[Printer-friendly Version](#)[Interactive Discussion](#)

diurnal cycles at the LHVP (Fig. 2). This cycle exhibits the same pattern as the  $\text{NO}_x$ ,  $\text{CO}_2$  and CO diurnal cycle, with maxima in the morning and at the end of the afternoon, which suggests the influence of traffic emissions on  $\text{NO}_x$  measurements. Traffic counts, provided by the Direction of Ile-de-France roads (DiRIF), are recorded for the main roads of the IdF region. The diurnal cycles of  $\text{CO}_2$  and CO at Trainou (180 m a.g.l.) present a single peak at noon on weekend and weekdays primarily reflecting the diurnal dynamics in the planetary boundary layer (PBL) as shown by Lopez et al. (2012) for radon-222 and nitrous oxide.

In Fig. 3, the diurnal cycles of  $\text{CO}_2$ , CO and  $\text{NO}_x$  that are recorded at the LHVP are plotted as functions of the air mass origin. The vertical lines are the standard deviation for each hour. As previously explained, the mean concentrations are generally higher when the air masses originate from the east, but the amplitudes of the morning peaks for the three species are similar for the two wind regimes. In contrast, the afternoon peaks in the oceanic wind regimes are more marked for  $\text{CO}_2$ , CO and  $\text{NO}_x$  than are those of the continental regime. In the oceanic wind regime, the LHVP is more sensitive to local pollution, which increases between 16:00 UTC and 18:00 UTC due to the traffic rush hour and the decrease in the PBL height. The signals decrease at the end of traffic rush hour as the atmosphere is refreshed by relatively clean air masses from the west. This second peak is less marked during the continental regime because the atmosphere is subsequently refreshed by the polluted air masses coming from east of Paris.

At the LHVP, non-methane hydrocarbons including benzene and toluene were monitored using gas chromatography coupled with an ionisation flame detector (see Gros et al., 2011, for more details). Benzene and toluene have life-times of approximately 11 and 2 days, respectively (for an OH value of  $10^6$  molecules  $\text{cm}^{-3}$ , Atkinson et al., 2006), and are typically emitted by the same sources. The toluene to benzene ratio is therefore often used to determine the photochemical age of an air mass: the lower the ratio, the older the air mass. This ratio may therefore be used to specify whether the observed pollution originated from a local source or was subject to long-range transport.

**Winter  $\text{CO}_2$  emission  
in Paris**

M. Lopez et al.

[Title Page](#)[Abstract](#)[Introduction](#)[Conclusions](#)[References](#)[Tables](#)[Figures](#)[◀](#)[▶](#)[◀](#)[▶](#)[Back](#)[Close](#)[Full Screen / Esc](#)[Printer-friendly Version](#)[Interactive Discussion](#)

On 4 and 5 February (oceanic regime), the ratio of toluene to benzene was recorded as approximately 5, whereas on 9 and 10 February (continental regime), the ratio decreased to 2. This result indicates that during the oceanic regime, air masses arriving in Paris were primarily affected by local pollution, whereas during the continental regime, long-range pollution sources were an additional factor.

### 3.2 Calculating the fossil fuel CO<sub>2</sub> contribution using radiocarbon measurements

As shown in several studies (Levin et al., 2003; Gamnitzer et al., 2006), the amount of <sup>14</sup>CO<sub>2</sub> in atmospheric samples can be used to derive the contribution of fossil fuel CO<sub>2</sub> to the measured atmospheric CO<sub>2</sub> mole fraction. The measured CO<sub>2</sub> mole fraction (CO<sub>2</sub>meas) is assumed to consist of a background CO<sub>2</sub> (CO<sub>2</sub>bg), a biospheric component (CO<sub>2</sub>bio) and a fossil fuel (CO<sub>2</sub>ff) component:

$$\text{CO}_2\text{meas} = \text{CO}_2\text{bg} + \text{CO}_2\text{ff} + \text{CO}_2\text{bio} \quad (2)$$

Each component has a characteristic  $\Delta^{14}\text{C}$  value.  $\Delta^{14}\text{Cff}$  is equal to  $-1000\text{‰}$  (free of <sup>14</sup>C), while  $\Delta^{14}\text{Cbio}$  can be measured remotely (or assumed).  $\Delta^{14}\text{Cbio}$  is equivalent to  $\Delta^{14}\text{Cbg}$  as  $\Delta^{14}\text{Cbio}$  includes a correction for mass dependent fractionation. Equation (3) is then derived as follows:

$$\text{CO}_2\text{ff} = \text{CO}_2\text{meas} \times \frac{\Delta^{14}\text{Cbg} - \Delta^{14}\text{Cmeas}}{\Delta^{14}\text{Cbg} + 1000} \quad (3)$$

In Eq. (3), other contributions to the <sup>14</sup>CO<sub>2</sub> budget such as the terrestrial disequilibrium isoflux due to heterotrophic respiration (Turnbull et al., 2006; Miller et al., 2012) and <sup>14</sup>CO<sub>2</sub> production from the nuclear power and reprocessing sector (Graven and Gruber, 2011) have been neglected.

In this study, Eq. (3) is applied to the flasks sampled at the LHVP and Jussieu station to quantify the contribution of fossil fuel CO<sub>2</sub> to the ambient air in Paris. The background

Title Page

Abstract

Introduction

Conclusions

References

Tables

Figures

◀

▶

◀

▶

Back

Close

Full Screen / Esc

Printer-friendly Version

Interactive Discussion



value of  $\Delta^{14}\text{C}_{\text{bg}}$  is derived from  $^{14}\text{CO}_2$  measurement at Mace Head (Ireland,  $53^\circ 19' \text{N}$ ,  $9^\circ 54' \text{W}$ , 25 m a.s.l.), which is considered a background site for Europe. In February 2010, the mean  $^{14}\text{CO}_2$  and  $\text{CO}_2$  values at Mace Head (wind selected for the oceanic sector, Bousquet et al., 1996) were 43.7‰ (I. Levin, personal communication, 2011) and 393.5 ppm, respectively. The analysis of the flasks yielded  $\Delta^{14}\text{C}_{\text{meas}}$  between  $-54.04\text{‰}$  and  $+15.59\text{‰}$  and a resulting  $\text{CO}_2\text{ff}$  contribution of 10.9 ppm to 41.9 ppm relative to the background air at Mace Head.

Figure 4 presents an example of a typical measurement day, 4 February 2010, at the LHVP. The one-minute averaged  $\text{CO}_2$  mole fractions obtained via continuous measurement are plotted in orange, and the  $\text{CO}_2$  mole fractions obtained from the flask measurements are indicated with red crosses. The background  $\text{CO}_2$  mole fraction at Mace Head during the maritime background conditions for February 2010 is plotted in blue.

Combining the  $\text{CO}_2$  and  $\Delta^{14}\text{CO}_2$  measurements from the individual flask samples permits us to determine the contribution of  $\text{CO}_2\text{ff}$  and  $\text{CO}_2\text{bio}$  to the observed  $\text{CO}_2$  mole fraction following Eq. (2). Fossil fuel  $\text{CO}_2$  (in grey) and biogenic  $\text{CO}_2$  (in green) are plotted in Fig. 4 using the right axis, which has the same amplitude as the left axis. Fossil fuel  $\text{CO}_2$  increases by 22.7 ppm from 07:15 to 08:15 UTC to reach a maximum of 41.9 ppm. Subsequently, we observe a small decrease until 12:00 UTC followed by a strong decrease (17.0 ppm) to 17.2 ppm at 13:00 UTC. The  $\text{NO}_x$  cycle (not shown) follows the same pattern, suggesting that local traffic contributes to the  $\text{CO}_2\text{ff}$  signal in the centre of Paris. The morning  $\text{CO}_2\text{ff}$  increase is due to the morning rush hour, and the subsequent decrease indicates the reduction in traffic as well as the PBL development. The figures for  $\text{CO}_2\text{bio}$  are lower (0–10 ppm) and exhibit less variation than those of  $\text{CO}_2\text{ff}$ . The same diurnal cycles are observed for  $\text{CO}_2\text{ff}$  and  $\text{CO}_2\text{bio}$  for the four sampling days at the LHVP and the single sampling day at Jussieu. Table 3 summarises the daily averages for  $\text{CO}_2\text{ff}$  and  $\text{CO}_2\text{bio}$  for each sampling day. The fossil fuel  $\text{CO}_2$  enhancement with respect to the background varies from 16.2 ppm to 32.8 ppm, and the biospheric  $\text{CO}_2$  contribution varies from 4.5 to 10.2 ppm. The differences in the

Winter  $\text{CO}_2$  emission  
in Paris

M. Lopez et al.

Title Page

Abstract

Introduction

Conclusions

References

Tables

Figures

◀

▶

◀

▶

Back

Close

Full Screen / Esc

Printer-friendly Version

Interactive Discussion



CO<sub>2</sub>ff and CO<sub>2</sub>bio mole fractions at the LHVP and Jussieu sites as they were observed on February 10 are related to the sampling period and location. During an airborne campaign over Sacramento in February 2009, Turnbull et al. (2011) determined that the contributions of CO<sub>2</sub>ff and CO<sub>2</sub>bio are as high as 8.6 and 8.0 ppm, respectively. In the present study, the greater CO<sub>2</sub>ff likely results from the fact that the samples were obtained closer to the surface and, thus, closer to the fossil fuel sources.

The contributions of the two CO<sub>2</sub> sources (fossil fuel and biogenic) to the CO<sub>2</sub>meas variability show that the majority of this variability is due to the injection of CO<sub>2</sub>ff into the atmosphere. On average, 77 % of the observed signal is caused by CO<sub>2</sub>ff (Table 3), mainly from road traffic, heating, and the residential sectors (AirParif). However, even in winter in a large city like Paris, the biospheric contribution of CO<sub>2</sub> fluxes was significant (23 % on average). This positive biospheric contribution can be attributed to net plant and soil respiration but also to the use of biofuel and to human respiration, which cannot be identified using <sup>14</sup>CO<sub>2</sub> measurement because these sources have been fixed or metabolised recently and have isotopic signatures that are similar to that of the ambient atmosphere. According to an AirParif emission inventory, CO<sub>2</sub> emissions from wood burning used for residential heating contribute less than 1 % of the total emissions in Paris and likely do not contribute significantly to the observed CO<sub>2</sub>bio enhancement. By 2009, the biofuel (ethanol) ratios in gasoline and diesel had increased to up to 10 % in France, which suggests that road traffic sources contribute significantly to the CO<sub>2</sub>bio results. AirParif estimates that the contribution of CO<sub>2</sub> from traffic is 17 % of the total fossil fuel CO<sub>2</sub> emissions for January 2008 after the emissions associated with ethanol in gasoline and diesel have been removed. According to our mean results for CO<sub>2</sub>ff and CO<sub>2</sub>bio as presented in Table 3, this contribution corresponds to an average CO<sub>2</sub>ff of 5 ppm from traffic. Because gasoline and diesel contain up to 10 % ethanol, the CO<sub>2</sub>bio enhancement due to traffic sources is 0.5 ppm or, approximately 15 % of the CO<sub>2</sub>bio in Paris during the winter. This could explain the covariance of CO<sub>2</sub>ff and CO<sub>2</sub>bio as observed in Fig. 4. A study by Turnbull et al. (2011) determined that the

**Winter CO<sub>2</sub> emission  
in Paris**

M. Lopez et al.

Title Page

Abstract

Introduction

Conclusions

References

Tables

Figures

◀

▶

◀

▶

Back

Close

Full Screen / Esc

Printer-friendly Version

Interactive Discussion



use of biofuels contributed up to 1 ppm of the positive CO<sub>2</sub>bio signal when gasoline required approximately 8 % ethanol in California.

A study by Ciais et al. (2007) shows that CO<sub>2</sub> emissions from human respiration in densely populated cities can reach 20 % of fossil fuel CO<sub>2</sub> emissions. Koerner and Klopatek (2002) show that human respiration is 500 kg CO<sub>2</sub> per year per person on average. With a population of 2.2 million in the centre of Paris, human respiration in the centre may be responsible for CO<sub>2</sub> emissions of approximately 1100 kt yr<sup>-1</sup>. By comparing this value to the reported fossil fuel CO<sub>2</sub> emissions of 7218 kt for the year 2005 in Paris reported by AirParif, human respiration contributes 15 % of the CO<sub>2</sub>ff emissions and this percentage is similar to the value reported in Ciais et al. (2007). Human respiration should be responsible for approximately 4 ppm of the CO<sub>2</sub> enhancement, and may therefore account for approximately 50 % of the CO<sub>2</sub>bio calculated. Finally, the last 35 % of CO<sub>2</sub>bio enhancement can be attributed to net plant and soil respiration. These values are only representative for our sampling sites at the LHVP and Jussieu for February 2010.

### 3.3 Separation of fossil fuel CO<sub>2</sub> sources using δ<sup>13</sup>C measurements

Several studies (Zondervan and Meijer, 1996; Meijer et al., 1996; Djuricin et al., 2010) have used <sup>13</sup>C/<sup>12</sup>C ratios in combination with <sup>14</sup>C measurements to quantify the fractions of emissions by different fossil fuel sources. Tans (1981) estimated that the release of CO<sub>2</sub> via anthropogenic combustion implies an average worldwide δ<sup>13</sup>C emissions for natural gas (δ<sup>13</sup>Cgas), liquid (δ<sup>13</sup>Cliq) and solid (δ<sup>13</sup>Csol) fuel of -41.0 ‰, -26.5 ‰ and -24.1 ‰, respectively. More recently, Andres et al. (2000) has shown that δ<sup>13</sup>C signatures depend on the geographic origin of fossil fuels and can range from -19 ‰ to -35 ‰ for liquids and from -20 ‰ to -100 ‰ for natural gas. A study by Widory and Javoy (2003) conducted direct δ<sup>13</sup>C measurements using exhaust gases from the main pollution sources in Paris. The authors determined that the mean δ<sup>13</sup>C source ratio for natural gas, liquid fuel and coal is -39.1 ± 1.1 ‰, -28.9 ± 0.4 ‰ and -24.8 ± 0.4 ‰, respectively. Based on the atmospheric δ<sup>13</sup>C and CO<sub>2</sub> measurements,

## Winter CO<sub>2</sub> emission in Paris

M. Lopez et al.

Title Page

Abstract

Introduction

Conclusions

References

Tables

Figures

◀

▶

◀

▶

Back

Close

Full Screen / Esc

Printer-friendly Version

Interactive Discussion



we estimate the signatures of the main  $\delta^{13}\text{C}$  sources, using a Keeling plot (Keeling, 1958, 1961; Pataki et al., 2003) for the daily observations. Assuming mass conservation and following Eq. (2) above, we derive Eq. (4), where  $\text{CO}_2\text{s}$  represents the sum of the  $\text{CO}_2$  sources (i.e.  $\text{CO}_2\text{s} = \text{CO}_2\text{ff} + \text{CO}_2\text{bio}$ ). Combining Eqs. (2) and (4), we obtain Eq. (5). We compute the relationship between  $\delta^{13}\text{C}_{\text{meas}}$  and the inverse mole fraction of the corresponding  $\text{CO}_2$  using a least squares method, following Pataki et al. (2003). The intercept corresponds to the mean signature of the source:  $\delta^{13}\text{C}_{\text{s}}$  (i.e. the last term of Eq. (5)). These values have been corrected for biospheric  $\delta^{13}\text{C}$  emission, assuming that  $\delta^{13}\text{C}_{\text{bio}} = -24.7\text{‰}$  (Bakwin et al., 1998), resulting in  $\delta^{13}\text{C}_{\text{ff}}$ .

$$\delta^{13}\text{C}_{\text{meas}} \times \text{CO}_2\text{meas} = \delta^{13}\text{C}_{\text{bg}} \times \text{CO}_2\text{bg} + \delta^{13}\text{C}_{\text{s}} \times \text{CO}_2\text{s} \quad (4)$$

$$\delta^{13}\text{C}_{\text{meas}} = \frac{\text{CO}_2\text{bg} \times (\delta^{13}\text{C}_{\text{bg}} - \delta^{13}\text{C}_{\text{s}})}{\text{CO}_2\text{meas}} + \delta^{13}\text{C}_{\text{s}} \quad (5)$$

At LHVP and Jussieu station, based on the data from the flasks sampled during the entire measurement period,  $\delta^{13}\text{C}_{\text{ff}}$  was equal to  $-36.1 \pm 2.7\text{‰}$  and  $-36.2 \pm 1.1\text{‰}$ , respectively, where the errors are the uncertainty in the intercept in Eq. (5). According to AirParif, the use of coal in the Paris region accounts for less than 1% of the total anthropogenic  $\text{CO}_2$  emission; thus, we will neglect this source. Using the  $\delta^{13}\text{C}_{\text{gas}}$  and  $\delta^{13}\text{C}_{\text{liq}}$  values measured by Widory and Javoy (2003) and the  $\delta^{13}\text{C}_{\text{ff}}$  source values from the Keeling plots yielded percentages of  $70 \pm 6\%$  for natural gas and  $30 \pm 3\%$  for liquid fuel. The emission inventory for Paris for 2008 that was provided by AirParif (described in Sect. 3.5) estimates the contribution of natural gas to be 37% of the total  $\text{CO}_2$  emissions.

We surmise that the higher ratio of gas consumption derived using the atmospheric method ( $70 \pm 6\%$ ) compared to the AirParif emission inventory (37%) likely arose from the spatial separation of automotive and residential sources and the lack of complete mixing prior to the sampling at our sampling location. We conducted our sampling during only a few days in winter, whereas the fraction provided by AirParif takes into

## Winter $\text{CO}_2$ emission in Paris

M. Lopez et al.

Title Page

Abstract

Introduction

Conclusions

References

Tables

Figures

◀

▶

◀

▶

Back

Close

Full Screen / Esc

Printer-friendly Version

Interactive Discussion



account data from entire year. We expected a higher fraction of gas consumption during the winter due to enhanced heating use. The  $\delta^{13}\text{C}$  flask measurements conducted on three days (9, 10 and 15 February 2010) by the IRMS show a mean  $\delta^{13}\text{C}_{\text{ff}}$  of  $-36.8 \pm 1.2\text{‰}$ . This value is slightly lower than the LHVP value, which suggests an even stronger influence of natural gas.

### 3.4 Constructing a continuous time series of fossil fuel $\text{CO}_2$

Precise  $^{14}\text{CO}_2$  measurements are difficult to perform and only are possible on discrete samples. Therefore, there are no direct methods of obtaining a continuous record of fossil fuel  $\text{CO}_2$ . To derive such a record for the entire campaign (defined here as FFCO<sub>2</sub>), we used two potential proxy tracers: carbon monoxide and  $\text{NO}_x$ . Both tracers are known to be typical proxies for fossil fuel combustion, but the emission ratios with respect to  $\text{CO}_2$  vary based on the combustion source. The daily ratios of each selected proxy to  $\text{CO}_2$  for the four days when we took  $^{14}\text{C}$  measurements at the LHVP site were used to construct the FFCO<sub>2</sub> curve. To compute the ratios  $R_{\text{CO}}$  and  $R_{\text{NO}_x}$ , defined here as  $\frac{\text{CO}}{\text{CO}_2\text{ff}} \times 1000$  and  $\frac{\text{NO}_x}{\text{CO}_2\text{ff}} \times 1000$ , we subtracted the background mole fraction from the ambient measurements. To ensure consistency, we chose to use the background CO mole fraction from the winter 2010 at Mace Head, which was equal to 121 ppb (Derwent et al., 2001, <http://agage.eas.gatech.edu/Stations/macehead.htm>). For  $\text{NO}_x$  background, we used a value of zero because of its short life-time (close to nine hours). The  $\text{CO}_2$  terms do not take into account the contribution of  $\text{CO}_2$  from ethanol use. To determine the FFCO<sub>2</sub> values, Eqs. (6) and (7) were used.

$$\text{FFCO}_2(\text{CO}) = \frac{\text{CO} - \text{CO}_{\text{bg}}}{R_{\text{CO}}} \quad (6)$$

$$\text{FFCO}_2(\text{NO}_x) = \frac{\text{NO}_x}{R_{\text{NO}_x}} \quad (7)$$

## Winter $\text{CO}_2$ emission in Paris

M. Lopez et al.

Title Page

Abstract

Introduction

Conclusions

References

Tables

Figures

◀

▶

◀

▶

Back

Close

Full Screen / Esc

Printer-friendly Version

Interactive Discussion



The emissions ratios for each of the four days of measurements at the LHVP are presented in Table 4 along with their respective coefficients of determination ( $r^2$ ). We observe that the ratios are functions of the wind regime (Table 4), with higher values on 4 and 5 February (oceanic regime) than on 9 and 10 February (continental regime). An average ratio for each air mass regime is applied to the appropriate segments of the continuous measurements to compute the FFCO<sub>2</sub> for each regime. For the few days without clearly identified air mass origin, we use the mean value from the two synoptic situations (Table 4).

In the upper panel of Fig. 5, we present the two curves inferred from  $R_{CO}$  and  $R_{NO_x}$ : FFCO<sub>2</sub>(CO) and FFCO<sub>2</sub>(NO<sub>x</sub>), respectively. The estimated FFCO<sub>2</sub> is greater during the continental wind regime: up to 80 ppm at three different times. In contrast, during the oceanic regime, the FFCO<sub>2</sub> mole fractions never exceed 40 ppm. At the bottom of Fig. 5, the FFCO<sub>2</sub>(CO) and FFCO<sub>2</sub>(NO<sub>x</sub>) mean diurnal cycles are plotted. These plots show the same pattern: a peak during the morning in the rush hour and a second peak at the end of afternoon. The FFCO<sub>2</sub>(CO) and FFCO<sub>2</sub>(NO<sub>x</sub>) mean mole fractions are 20.6 ppm and 18.7 ppm, respectively. Differences are observed during the evening and over night (from 17:00 UTC until 06:00 UTC) because of the short life-time of NO<sub>x</sub> relative to the life-time of CO.

A study by Vogel et al. (2010) shows that  $R_{CO}$  has a diurnal cycle because anthropogenic CO<sub>2</sub> (and CO) fluxes are subject to strong diurnal variation. During the winter, the authors found a peak-to-peak amplitude of 8 ppb ppm<sup>-1</sup>, with the lowest ratio at 08:00 UTC and the highest at 18:00 UTC. We assume a constant ratio during the day in this study.

### 3.5 Comparison of $R_{CO}$ and $R_{NO_x}$ ratios with emission inventories

In this section, we compare the  $R_{CO}$  and  $R_{NO_x}$  emission ratios measured in Paris with those derived from implied emission inventories. Four different emission inventories are presented with different spatial and temporal resolutions. The reference years for the inventories vary from 2005 to 2010, which makes it difficult to compare the ratios

## Winter CO<sub>2</sub> emission in Paris

M. Lopez et al.

[Title Page](#)[Abstract](#)[Introduction](#)[Conclusions](#)[References](#)[Tables](#)[Figures](#)[◀](#)[▶](#)[◀](#)[▶](#)[Back](#)[Close](#)[Full Screen / Esc](#)[Printer-friendly Version](#)[Interactive Discussion](#)

directly. For France as a whole, CITEPA has calculated the GHG emissions on a yearly basis since 1960. In addition, AirParif provides a regional inventory for the IdF with a spatial resolution of  $1 \times 1$  km. AirParif assessed the  $\text{CO}_2$  and  $\text{NO}_x$  emissions with a one-hour time resolution for three typical days (weekdays, Saturdays and Sundays) in January 2008. The Institute for Energy Economics and the Rational Use of Energy (IER, 2005) has provided a European inventory with a resolution of  $1 \times 1$  min for France for the year 2005. EDGAR 4.2 is a global inventory of GHG emissions and has reported annual values for France since 1970. EDGAR 4.2 also provides a gridded version with a resolution of  $0.1 \times 0.1$  degree for the reference year 2008 (Olivier et al., 2001; Olivier and Berdowsky, 2001). The spatial resolution of IER and AirParif allowed us to extract the exact grid cells that corresponded to Paris, whereas for EDGAR 4.2, we chose the grid cell that included most of the Paris area.

The ratios for each inventory are presented in Table 5 for different reference years, spatial and time resolutions. For France as a whole, CITEPA estimates a higher  $R_{\text{CO}}$  ratio than does EDGAR 4.2, whereas the ratios are similar for  $R_{\text{NO}_x}$ . For Paris, EDGAR 4.2 shows much lower  $R_{\text{CO}}$  ratios (4.3) than does the IER inventory (14.6). The  $R_{\text{NO}_x}$  ratios vary substantially across the different emission inventories; they are 3.9 (EDGAR 4.2), 3.0 (IER) and 2.1 (AirParif). These differences are due to discrepancies in the sources spatial descriptions for Paris and to the different ratios used for the same source sectors in different inventories. These large differences between inventories suggest that more work must be conducted to provide more consistent estimates.

In Table 6, we summarised the percentage contributions of the three main source sectors (road transport, residential and industry) as well as the  $R_{\text{CO}}$  and  $R_{\text{NO}_x}$  ratios for the different sectors for the different inventories. On a the French scale, the  $R_{\text{CO}}$  and  $R_{\text{NO}_x}$  ratios stayed fairly constant between 2005 and 2010 except for the road transport ratio. The  $R_{\text{CO}}$  ratio for road transport decreased by a factor of two in five years. This decrease is primarily a function of the environmental policy applied to road vehicles since 1970 and is also an effect of the adoption and improvement of catalytic converters for vehicles since 1993, which has reduced  $\text{NO}_x$  and particularly CO emissions. The large

Winter  $\text{CO}_2$  emission  
in Paris

M. Lopez et al.

[Title Page](#)[Abstract](#)[Introduction](#)[Conclusions](#)[References](#)[Tables](#)[Figures](#)[◀](#)[▶](#)[◀](#)[▶](#)[Back](#)[Close](#)[Full Screen / Esc](#)[Printer-friendly Version](#)[Interactive Discussion](#)

decrease in  $R_{CO}$  that is associated with road transport explains the difference between the EDGAR 4.2 ( $R_{CO} = 4.3$ ) and IER ( $R_{CO} = 14.6$ ) figures because these ratios are not based on the same reference year and because EDGAR 4.2 estimates a high contribution to road transport for  $CO_2$  emissions. In France overall, the different  $R_{CO}$  ratios for industrial sources reported by CITEPA and EDGAR 4.2 explain the difference in their total  $R_{CO}$  ratio. We are more confident in the lower range of  $R_{CO}$  values for the industry sector because the industry sector has more efficient combustion and catalytic systems than does the residential sector.

The  $R_{NO_x}$  ratios estimated by the four inventories for the road transport sector are consistent. For the residential and industrial sectors, EDGAR 4.2 estimates the highest ratios, which explains the high total ratio, whereas AirParif estimates small residential and industrial sector ratios and thus derives the lowest total ratio. For Paris, EDGAR 4.2 estimates that the road transport sector is a more important  $CO_2$  source than the other inventories. The contribution of the road transport sector is the lowest for the AirParif inventory. The selected month (January) for this inventory, is associated with a stronger contribution by residential sources due to heating, which reduces the relative contribution of the road transport and industrial sectors.

We compared the ratios determined using our top-down atmospheric approach (Table 4) with the available inventories (Tables 5 and 6). We focus first on the  $R_{CO}$  ratio and then on the  $R_{NO_x}$  ratio. During oceanic regimes, our mean  $R_{CO}$  ratio of 13 is similar to the ratios from IER and CITEPA (Table 5). These high ratios are representative of the residential sector (Table 6). This result is consistent with the ratio of benzene to toluene that we found in part 3 which indicates that our samples are sensitive to local emissions during the oceanic regime. Our  $R_{CO}$  ratio for the continental regime is 8.5 and lies between the IER and CITEPA estimates and those of EDGAR 4.2. According to the AirParif inventory, the north and northeastern areas of Paris have relatively significant  $CO_2$  emissions from industrial sources (approximately 20 % of anthropogenic  $CO_2$ ) compared with southern Paris (less than 5 % of anthropogenic  $CO_2$ ). This result is in agreement with the ratio that we found for the continental regime, which indicates

**Winter  $CO_2$  emission  
in Paris**

M. Lopez et al.

Title Page

Abstract

Introduction

Conclusions

References

Tables

Figures

◀

▶

◀

▶

Back

Close

Full Screen / Esc

Printer-friendly Version

Interactive Discussion



**Winter CO<sub>2</sub> emission  
in Paris**

M. Lopez et al.

[Title Page](#)[Abstract](#)[Introduction](#)[Conclusions](#)[References](#)[Tables](#)[Figures](#)[◀](#)[▶](#)[◀](#)[▶](#)[Back](#)[Close](#)[Full Screen / Esc](#)[Printer-friendly Version](#)[Interactive Discussion](#)

that the contribution of the road transport and industry sectors, which have low  $R_{CO}$  ratios, are stronger. Moreover, the ratio of benzene to toluene during this regime indicated that long-range transport had occurred, which would have permitted the emissions from Benelux and Germany to have a greater influence. These are industrialised areas that are characterised by relatively low  $R_{CO}$  ratios relative to those of France (Gamnitzer et al., 2006). We noticed that EDGAR 4.2 found a much lower  $R_{CO}$  in Paris than did other inventories and that this figure was also much lower than our estimate. This difference is most likely due to the low  $R_{CO}$  ratio of 1.0 for the residential sector for the grid cell for Paris relative to the high value of 15.1 for France.

Because of its short life-time, the  $R_{NO_x}$  ratio is less sensitive to contributions from different sources. Nevertheless, the ratios we found are within the range of the inventory estimates. During the continental regime,  $NO_x$  destroyed during transport over the continent, which leads to lower  $R_{NO_x}$  values. In the oceanic regime, the high ratios show the contribution of the road transport sector near the station.

## 4 Conclusions

This pilot study has demonstrated that measurement of the  $CO_2$  and the CO mole fraction together with isotopic  $CO_2$  measurements can help to better quantify the fossil fuels component in cities. Radiocarbon measurements taken using flask sampling allowed us to directly derive the fossil fuel  $CO_2$  mole fraction in Paris, which was in February 2010 approximately 20 ppm (on average). Of the total  $CO_2$  enhancement in Paris during this period, 77 % can be attributed to anthropogenic sources ( $CO_{2ff}$ ) and 23 % to biospheric sources ( $CO_{2bio}$ ). Using values from the literature, we estimated that half of these biospheric emissions are due to human respiration and that the other half are due to soil respiration (35 %) and the use of ethanol in gasoline and diesel (15 %).

Making use of  $\delta^{13}C$  measurements, we were able to determine the contributions of natural gas and liquid fuel to anthropogenic  $CO_2$  emissions, which amounted to 70 %

and 30 %, respectively. This estimation was possible in Paris because we have only two sources of fossil fuel emissions; the use of coal can be neglected because it produces less than 1 % of the total CO<sub>2</sub> emission. This calculation would be even more powerful, if we could reduce the errors generated by the isotopic source signature of natural gas, which varies according to the supply of natural gas (i.e. whether it originates in Siberia or the North Sea). During future campaigns, it would be helpful to measure the source signature of natural gas from the gas supply network on a regular basis.

Carbon monoxide and nitrogen oxides, which were monitored continuously, were successfully used as proxies to determine the anthropogenic CO<sub>2</sub> emissions over the entire campaign. These proxies have been calibrated against the  $\frac{\text{CO}}{\text{CO}_{2\text{ff}}}$  and  $\frac{\text{NO}_x}{\text{CO}_{2\text{ff}}}$  ratios. We determined that the ratios change as a function of the air mass origin. Therefore, it was possible to use different ratios for the proxies depending on the air mass regime. The data for the  $\frac{\text{CO}}{\text{CO}_{2\text{ff}}}$  and  $\frac{\text{NO}_x}{\text{CO}_{2\text{ff}}}$  ratios are consistent with the information from the inventories although there are sizeable variations across the inventories themselves. According to these inventories, during the oceanic regime, we are more sensitive to the emissions from the residential sector, the  $\frac{\text{CO}}{\text{CO}_{2\text{ff}}}$  ratio is high. During the continental regime, that ratio decreases, showing the increase in the influence of the road transport and industrial sectors.

*Acknowledgements.* We thank the MEGAPOLI project that allowed us to place our instruments at LHVP during the winter campaign 2010. We used NO<sub>x</sub> data from the MEGAPOLI Database which were founded by the European Union's Seventh Framework Programme FP/2007-2011 within the project MEGAPOLI, grant agreement n°212520. We thank François Truong, Cyrille Vuillemin and Vincent Bazantay from LSCE/RAMCES for maintaining the instrumentation during the campaign and performing the flasks analysis. We thank Ingeborg Levin for providing <sup>14</sup>C measurement at Mace Head as well as Yao Té and Pascal Jeseck for the meteorological data for the Jussieu site. We want to thank Claude Camy-Peyret for his occasional help during the campaign with TDL spectrometer and Laurence Croizé for the instrumental development. We also thank Balendra Thiruchittampalam for the helpful discussions about IER inventory. This work was supported partly by ANR-CO<sub>2</sub>-MegaParis project, GHG-Europe, CNRS and CEA.

**Winter CO<sub>2</sub> emission  
in Paris**

M. Lopez et al.

Title Page

Abstract

Introduction

Conclusions

References

Tables

Figures

◀

▶

◀

▶

Back

Close

Full Screen / Esc

Printer-friendly Version

Interactive Discussion



The publication of this article is financed by CNRS-INSU.

## References

- Andres, R. J., Marland, G., Boden, T., and Bischof, S.: Carbon dioxide emissions from fossil fuel consumption and cement manufacture, 1751–1991, and an estimate of their isotopic composition and latitudinal distribution, *The carbon cycle*, 62, 53–62, New York, 2000. 2389
- Atkinson, R., Baulch, D. L., Cox, R. A., Crowley, J. N., Hampson, R. F., Hynes, R. G., Jenkin, M. E., Rossi, M. J., Troe, J., and IUPAC Subcommittee: Evaluated kinetic and photochemical data for atmospheric chemistry: Volume II – gas phase reactions of organic species, *Atmos. Chem. Phys.*, 6, 3625–4055, doi:10.5194/acp-6-3625-2006, 2006. 2383, 2385
- Bakwin, P. S., Tans, P. P., White, J. W. C., and Andres, R. J.: Determination of the isotopic  $^{13}\text{C}/^{12}\text{C}$  discrimination by terrestrial biology from a global network of observations, *Global Biogeochem. Cy.*, 12, 555–562, 1998. 2390
- Bousquet, P., Gaudry, A., Ciais, P., Kazan, V., Monfray, P., Simmonds, P. G., Jennings, S., and O'Connor, T.: Atmospheric  $\text{CO}_2$  concentration variations recorded at Mace Head, Ireland, from 1992 to 1994, *Phys. Chem. Earth*, 21, 477–481, 1996. 2387
- Bousquet, P., Peylin, P., Ciais, P., Le Quéré, C., Friedlingstein, P., and Tans, P. P.: Regional changes in carbon dioxide fluxes of land and oceans since 1980, *Science*, 290, 1342–1346, 2000. 2374
- Bousquet, P., Ciais, P., Miller, J. B., Dlugokencky, E. J., Hauglustaine, D. A., Prigent, C., Van der Werf, G. R., Peylin, P., Brunke, E. G., Carouge, C., Langenfelds, R. L., Lathiere, J., Papa, F., Ramonet, M., Schmidt, M., Steele, L. P., Tyler, S. C., and White, J.: Contribution of anthropogenic and natural sources to atmospheric methane variability, *Nature*, 443, 439–443, 2006. 2375

## Winter $\text{CO}_2$ emission in Paris

M. Lopez et al.

Title Page

Abstract

Introduction

Conclusions

References

Tables

Figures

◀

▶

◀

▶

Back

Close

Full Screen / Esc

Printer-friendly Version

Interactive Discussion



## Winter CO<sub>2</sub> emission in Paris

M. Lopez et al.

Title Page

Abstract

Introduction

Conclusions

References

Tables

Figures

◀

▶

◀

▶

Back

Close

Full Screen / Esc

Printer-friendly Version

Interactive Discussion



Ciais, P., Bousquet, P., Freibauer, A., and Naegler, T.: Horizontal displacement of carbon associated with agriculture and its impacts on atmospheric CO<sub>2</sub>, *Global Biogeochem. Cy.*, 21, GB2014, doi:10.1029/2006GB002741, 2007. 2389

CITEPA: Rapport national d'inventaire pour la France au titre de la convention cadre des Nations Unies sur les changements climatiques et du protocole de Kyoto, 2012. 2374

Croizé, L., Mondelain, D., Camy-Peyret, C., Janssen, C., Lopez, M., Delmotte, M., and Schmidt, M.: Isotopic composition and concentration measurements of atmospheric CO<sub>2</sub> with a diode laser making use of correlations between non-equivalent absorption cells, *Appl. Phys. B-Lasers O.*, 101, 411–421, 2010. 2378, 2380, 2382

Derwent, R. G., Ryall, D. B., Jennings, S. G., Spain, T. G., and Simmonds, P. G.: Black carbon aerosol and carbon monoxide in European regionally polluted air masses at Mace Head, Ireland during 1995–1998, *Atmos. Environ.*, 35, 6371–6378, 2001. 2391

Djuricin, S., Pataki, D. E., and Xu, X.: A comparison of tracer methods for quantifying CO<sub>2</sub> sources in an urban region, *J. Geophys. Res.*, 115, D11303, doi:10.1029/2009JD012236, 2010. 2389

Dolgorouky, C., Gros, V., Sarda-Esteve, R., Sinha, V., Williams, J., Marchand, N., Sauvage, S., Poulain, L., Sciare, J., and Bonsang, B.: Total OH reactivity measurements in Paris during the 2010 MEGAPOLI winter campaign, *Atmos. Chem. Phys.*, 12, 9593–9612, doi:10.5194/acp-12-9593-2012, 2012. 2376

Duren, R. M. and Miller, C. E.: Measuring the carbon emissions of megacities, *Nature Climate Change*, 2, 560–562, 2012. 2373, 2375

Gamitzer, U., Karstens, U., Kromer, B., Neubert, R. E. M., Meijer, H. A. J., Schroeder, H., and Levin, I.: Carbon monoxide: A quantitative tracer for fossil fuel CO<sub>2</sub>, *J. Geophys. Res.*, 111, D22302, doi:10.1029/2005JD006966, 2006. 2386, 2395

Graven, H. D. and Gruber, N.: Continental-scale enrichment of atmospheric <sup>14</sup>CO<sub>2</sub> from the nuclear power industry: potential impact on the estimation of fossil fuel-derived CO<sub>2</sub>, *Atmos. Chem. Phys.*, 11, 12339–12349, doi:10.5194/acp-11-12339-2011, 2011. 2386

Gros, V., Gaimoz, C., Herrmann, F., Custer, T., Williams, J., Bonsang, B., Sauvage, S., Locoge, N., d'Argouges, O., Sarda-Estève, R., and Sciare, J.: Volatile organic compounds sources in Paris in spring 2007. Part I: Qualitative analysis, *Environ. Chem.*, 8, 74–90, 2011. 2385

Haefelin, M., Barthès, L., Bock, O., Boitel, C., Bony, S., Bouniol, D., Chepfer, H., Chiriaco, M., Cuesta, J., Delanoë, J., Drobinski, P., Dufresne, J.-L., Flamant, C., Grall, M., Hodzic, A., Hourdin, F., Lapouge, F., Lemaître, Y., Mathieu, A., Morille, Y., Naud, C., Noël, V., O'Hirok, W.,

**Winter CO<sub>2</sub> emission  
in Paris**

M. Lopez et al.

Title Page

Abstract

Introduction

Conclusions

References

Tables

Figures

◀

▶

◀

▶

Back

Close

Full Screen / Esc

Printer-friendly Version

Interactive Discussion



- Pelon, J., Pietras, C., Protat, A., Romand, B., Scialom, G., and Vautard, R.: SIRTA, a ground-based atmospheric observatory for cloud and aerosol research, *Ann. Geophys.*, 23, 253–275, doi:10.5194/angeo-23-253-2005, 2005. 2378
- 5 Hammer, S. and Levin, I.: Seasonal variation of the molecular hydrogen uptake by soils inferred from continuous atmospheric observations in Heidelberg, southwest Germany, *Tellus B*, 61, 556–565, 2009. 2375
- Healy, R. M., Sciare, J., Poulain, L., Kamili, K., Merkel, M., Müller, T., Wiedensohler, A., Eckhardt, S., Stohl, A., Sarda-Estève, R., McGillicuddy, E., O'Connor, I. P., Sodeau, J. R., and Wenger, J. C.: Sources and mixing state of size-resolved elemental carbon particles in a  
10 European megacity: Paris, *Atmos. Chem. Phys.*, 12, 1681–1700, doi:10.5194/acp-12-1681-2012, 2012. 2376
- Hirsch, A. I., Michalak, A. M., Bruhwiler, L. M., Peters, W., Dlugokencky, E. J., and Tans, P. P.: Inverse modeling estimates of the global nitrous oxide surface flux from 1998–2001, *Global Biogeochem. Cy.*, 20, GB1008, doi:10.1029/2004GB002443, 2006. 2375
- 15 IER: Emission data, <http://carboeurope.ier.uni-stuttgart.de> (last access: January 2013), 2005. 2393
- Kaiser, C., Schmidt, M., Lavric, J. V., Laurent, O., Vuillemin, C., Yver, C., and Ramonet, M.: Evaluation of five CO analysers, *Tech. rep.*, LSCE-CEA-CNRS-IPSL, Gif-sur-Yvette, 2010. 2380
- 20 Keeling, C. D.: The concentration and isotopic abundances of atmospheric carbon dioxide in rural areas, *Geochim. Cosmochim. Ac.*, 13, 322–334, 1958. 2390
- Keeling, C. D.: The concentration and isotopic abundances of carbon dioxide in rural and marine air, *Geochim. Cosmochim. Ac.*, 24, 277–298, 1961. 2390
- Koerner, B. and Klopatek, J.: Anthropogenic and natural CO<sub>2</sub> emission sources in an arid urban environment, *Environ. Pollut.*, 116, Supplement 1, S45–S51, doi:10.1016/S0269-7491(01)00246-9, 2002. 2389
- 25 Levin, I. and Karstens, U.: Inferring high-resolution fossil fuel CO<sub>2</sub> records at continental sites from combined <sup>14</sup>CO<sub>2</sub> and CO observations, *Tellus B*, 59, 245–250, 2007. 2375
- Levin, I., Kromer, B., Schmidt, M., and Sartorius, H.: A novel approach for independent budgeting of fossil fuel CO<sub>2</sub> over Europe by <sup>14</sup>CO<sub>2</sub> observations, *Geophys. Res. Lett.*, 30, 2194, doi:10.1029/2003GL018477, 2003. 2375, 2386
- 30 Lopez, M., Schmidt, M., Yver, C., Messenger, C., Worthy, D., Kazan, V., Ramonet, M., Bousquet, P., and Ciais, P.: Seasonal variation of N<sub>2</sub>O emissions in France inferred

- from atmospheric N<sub>2</sub>O and <sup>222</sup>Rn measurements, *J. Geophys. Res.*, 117, D14103, doi:10.1029/2012JD017703, 2012. 2378, 2379, 2380, 2385
- Meijer, H. A. J., Smid, H. M., Perez, E., and Keizer, M. G.: Isotopic characterisation of anthropogenic CO<sub>2</sub> emissions using isotopic and radiocarbon analysis, *Phys. Chem. Earth*, 21, 483–487, 1996. 2389
- Messenger, C.: Greenhouse gases regional fluxes estimated from atmospheric measurements, Ph. D. thesis, Université Paris 7 – Denis Diderot, available at: <http://tel.archives-ouvertes.fr/tel-00164720> (last access: January 2013), 2007. 2379, 2380
- Miller, J. B., Lehman, S. J., Montzka, S. A., Sweeney, C., Miller, B. R., Karion, A., Wolak, C., Dlugokencky, J., Southon, J., Turnbull, J. C., and Tans, P. P.: Linking emissions of fossil fuel CO<sub>2</sub> and other anthropogenic trace gases using atmospheric <sup>14</sup>CO<sub>2</sub>, *J. Geophys. Res.*, 117, D08302, doi:10.1029/2011JD017048, 2012. 2386
- Neubert, R. E. M., Spijkervet, L. L., Schut, J. K., Been, H. A., and Meijer, H. A. J.: A computer-controlled continuous air drying and flask sampling system, *J. Atmos. Ocean. Tech.*, 21, 651–659, 2004. 2377
- Olivier, J. G. J. and Berdowsky, J. J. M.: Global emissions sources and sinks, in: *The Climate System*, edited by: Berdowski, J., Guicherit, R., and Heij, B. J., 33–78. A.A. Balkema Publishers/Swets & Zeitlinger Publishers, Lisse, The Netherlands, ISBN 90 5809 255 0, 2001. 2374, 2393
- Olivier, J. G. J., Berdowski, J. J. M., Peters, J., Bakker, J., Visschedijk, A. J. H., and Bloos, J. P. J.: Applications of EDGAR. Including a description of EDGAR 3.0: reference database with trend data for 1970–1995, RIVM, Bilthoven. RIVM report no. 773301 001/ NOP report no. 410200 051, 2001. 2374, 2393
- Pataki, D. E., Ehleringer, J. R., Flanagan, L. B., Yakir, D., Bowling, D. R., Still, C. J., Buchmann, N., Kaplan, J. O., and Berry, J. A.: The application and interpretation of Keeling plots in terrestrial carbon cycle research, *Global Biogeochem. Cy.*, 17, 1022, doi:10.1029/2001GB001850, 2003. 2390
- Pépin, L., Schmidt, M., Ramonet, M., Worhty, D. E. J., and Ciais, P.: A new gas chromatographic experiment to analyse greenhouse gases in flask samples and ambient air in the region of Saclay, Tech. rep., IPSL, available at: [www.lmd.polytechnique.fr/nai/nai\\_27.pdf](http://www.lmd.polytechnique.fr/nai/nai_27.pdf), 2001. 2378
- Peylin, P., Rayner, P. J., Bousquet, P., Carouge, C., Hourdin, F., Heinrich, P., Ciais, P., and AEROCARB contributors: Daily CO<sub>2</sub> flux estimates over Europe from continuous at-

**Winter CO<sub>2</sub> emission  
in Paris**

M. Lopez et al.

Title Page

Abstract

Introduction

Conclusions

References

Tables

Figures

◀

▶

◀

▶

Back

Close

Full Screen / Esc

Printer-friendly Version

Interactive Discussion



ospheric measurements: 1, inverse methodology, *Atmos. Chem. Phys.*, 5, 3173–3186, doi:10.5194/acp-5-3173-2005, 2005. 2374

Peylin, P., Houweling, S., Krol, M. C., Karstens, U., Rödenbeck, C., Geels, C., Vermeulen, A., Badawy, B., Aulagnier, C., Pregger, T., Delage, F., Pieterse, G., Ciais, P., and Heimann, M.: Importance of fossil fuel emission uncertainties over Europe for CO<sub>2</sub> modeling: model intercomparison, *Atmos. Chem. Phys.*, 11, 6607–6622, doi:10.5194/acp-11-6607-2011, 2011. 2374

Rayner, P. and Law, R.: The interannual variability of the global carbon cycle, *Tellus B*, 51, 210–212, 1999. 2374

Rödenbeck, C.: Estimating CO<sub>2</sub> sources and sinks from atmospheric mixing ratio measurements using a global inversion of atmospheric transport, Tech. rep., MPI BGC, 2005. 2375

Rödenbeck, C., Houweling, S., Gloor, M., and Heimann, M.: CO<sub>2</sub> flux history 1982–2001 inferred from atmospheric data using a global inversion of atmospheric transport, *Atmos. Chem. Phys.*, 3, 1919–1964, doi:10.5194/acp-3-1919-2003, 2003. 2374

Royer, P., Chazette, P., Sartelet, K., Zhang, Q. J., Beekmann, M., and Raut, J. C.: Comparison of lidar-derived PM<sub>10</sub> with regional modeling and ground-based observations in the frame of MEGAPOLI experiment, *Atmos. Chem. Phys.*, 11, 10705–10726, doi:10.5194/acp-11-10705-2011, 2011. 2376

Schmidt, M., Ramonet, M., Wastine, B., Delmotte, M., Galdemard, P., Kazan, V., Messenger, C., Royer, A., Valant, C., Xueref, I., and Ciais, P.: RAMCES: The French Network of Atmospheric Greenhouse Gas Monitoring, in WMO/GAW report 168, in: The 13th WMO/IAEA Meeting of Experts on Carbon Dioxide Concentration and Related Tracers Measurement Techniques, 1359, 2005. 2381

Stohl, A., Burkhardt, J. F., Eckhardt, S., Hirdman, D., and Sodemann, H.: An integrated internet-based system for analyzing the influence of emission sources and atmospheric transport on measured concentrations of trace gases and aerosols, Tech. rep., NILU, Norway, 2007. 2383

Stuiver, M. and Polach, H. A.: Reporting of <sup>14</sup>C data, *Radiocarbon*, 19, 355–363, 1977. 2382

Tans, P. P.: <sup>13</sup>C/<sup>12</sup>C of industrial CO<sub>2</sub>, *Carbon Cycle Modelling*, SCOPE, 16, 127–129, 1981. 2389

Thompson, R. L., Gerbig, C., and Rödenbeck, C.: A Bayesian inversion estimate of N<sub>2</sub>O emissions for western and central Europe and the assessment of aggregation errors, *Atmos. Chem. Phys.*, 11, 3443–3458, doi:10.5194/acp-11-3443-2011, 2011. 2375

## Winter CO<sub>2</sub> emission in Paris

M. Lopez et al.

Title Page

Abstract

Introduction

Conclusions

References

Tables

Figures

◀

▶

◀

▶

Back

Close

Full Screen / Esc

Printer-friendly Version

Interactive Discussion



## Winter CO<sub>2</sub> emission in Paris

M. Lopez et al.

Title Page

Abstract

Introduction

Conclusions

References

Tables

Figures

◀

▶

◀

▶

Back

Close

Full Screen / Esc

Printer-friendly Version

Interactive Discussion



Turnbull, J. C., Miller, J. B., Lehman, S. J., Tans, P. P., Sparks, R. J., and Southon, J.: Comparison of <sup>14</sup>CO<sub>2</sub>, CO, and SF<sub>6</sub> as tracers for recently added fossil fuel CO<sub>2</sub> in the atmosphere and implications for biological CO<sub>2</sub> exchange, *Geophys. Res. Lett.*, 33, L01817, doi:10.1029/2005GL024213, 2006. 2375, 2386

5 Turnbull, J. C., Lehman, S. J., Miller, J. B., Sparks, R. J., Southon, J. R., and Tans, P. P.: A new high precision <sup>14</sup>CO<sub>2</sub> time series for North American continental air, *J. Geophys. Res.*, 112, D11310, doi:10.1029/2006JD008184, 2007. 2382

10 Turnbull, J. C., Karion, A., Fischer, M. L., Faloona, I., Guilderson, T., Lehman, S. J., Miller, B. R., Miller, J. B., Montzka, S., Sherwood, T., Saripalli, S., Sweeney, C., and Tans, P. P.: Assessment of fossil fuel carbon dioxide and other anthropogenic trace gas emissions from airborne measurements over Sacramento, California in spring 2009, *Atmos. Chem. Phys.*, 11, 705–721, doi:10.5194/acp-11-705-2011, 2011. 2388

15 van der Laan, S., Neubert, R. E. M., and Meijer, H. A. J.: Methane and nitrous oxide emissions in The Netherlands: ambient measurements support the national inventories, *Atmos. Chem. Phys.*, 9, 9369–9379, doi:10.5194/acp-9-9369-2009, 2009. 2375

Vogel, F. R., Hammer, S., Steinhof, A., Kromer, B., and Levin, I.: Implication of weekly and diurnal <sup>14</sup>C calibration on hourly estimates of CO-based fossil fuel CO<sub>2</sub> at a moderately polluted site in southwestern Germany, *Tellus B*, 62, 512–520, 2010. 2375, 2392

20 Wastine, B., Kaiser, C., Vuillelin, C., Lavric, J. V., Schmidt, M., and Ramonet, M.: Evaluation of the EnviroSense 3000i analysers for continuous CO<sub>2</sub>/CH<sub>4</sub> measurements by CRDS, Tech. rep., LSCE-CEA-CNRS-IPSL, 2009. 2379

Werner, R. A., Rothe, M., and Brand, W. A.: Extraction of CO<sub>2</sub> from air samples for isotopic analysis and limits to ultra high precision δ<sup>18</sup>O determination in CO<sub>2</sub> gas, *Rapid Commun. Mass Sp.*, 15, 2152–2167, 2001. 2381

25 Widory, D. and Javoy, M.: The carbon isotope composition of atmospheric CO<sub>2</sub> in Paris, *Earth Planet. Sci. Lett.*, 215, 289–298, 2003. 2389, 2390

WMO-GAW (Ed.): 13th WMO/IAEA Meeting of Experts on Carbon Dioxide, Other Greenhouse Gases, and Related Tracer Measurement Techniques, vol. 168, Global Atmosphere Watch, Boulder, Colorado, USA, 2005. 2378

30 WMO-GAW (Ed.): 15th WMO/IAEA Meeting of Experts on Carbon Dioxide, Other Greenhouse Gases, and Related Tracer Measurement Techniques, vol. 194, Global Atmosphere Watch, Jena, Germany, 2009. 2382

Yver, C., Schmidt, M., Bousquet, P., Zahorowski, W., and Ramonet, M.: Estimation of the molecular hydrogen soil uptake and traffic emissions at a suburban site near Paris through hydrogen, carbon monoxide, and radon-222 semicontinuous measurements, *J. Geophys. Res.*, 114, D18304, doi:10.1029/2009JD012122, 2009. 2375, 2378, 2380

5 Yver, C., Schmidt, M., Bousquet, P., and Ramonet, M.: Measurements of molecular hydrogen and carbon monoxide on the Trainou tall tower, *Tellus B*, 2010. 2379

Zondervan, A. and Meijer, H. A. J.: Isotopic characterisation of CO<sub>2</sub> sources during regional pollution events using isotopic and radiocarbon analysis, *Tellus B*, 48, 601–612, 1996. 2389

Winter CO<sub>2</sub> emission in Paris

M. Lopez et al.

Title Page

Abstract

Introduction

Conclusions

References

Tables

Figures

⏪

⏩

◀

▶

Back

Close

Full Screen / Esc

Printer-friendly Version

Interactive Discussion



## Winter CO<sub>2</sub> emission in Paris

M. Lopez et al.

**Table 1.** Technologies, models, locations and accuracy of instruments for the analysed species with the respective measurement dates.

Technology	Model	Location	Date	Species and accuracy
CRDS	Picarro G1302	LHVP	15 Jan 2010– 19 Feb 2010	CO <sub>2</sub> : 0.03 ppm; CO: 10.0 ppb
TDL	SIMCO	Jussieu	08 Feb 2010– 12 Feb 2010	CO <sub>2</sub> : 0.05 ppm; $\delta^{13}\text{C}$ : 0.15 ‰
GC (FID/ECD)	HP-6890	LSCE Trainou	15 Jan 2010– 19 Feb 2010	CO <sub>2</sub> : 0.05 ppm; CH <sub>4</sub> : 1.0 ppb N <sub>2</sub> O: 0.3 ppb; SF <sub>6</sub> : 0.05 ppt
GC (RGD)	Peak-Performer	LSCE Trainou	15 Jan 2010– 19 Feb 2010	CO: 1 ppb; H <sub>2</sub> : 2.0 ppb
Chemiluminescence	Environment SA AC31M	LHVP SIRTA	15 Jan 2010– 15 Feb 2010	NO <sub>x</sub> : 10 %
MS	Finigan MAT 252	LSCE	flasks	$\delta^{13}\text{C}$ : 0.02 ‰; $\delta^{18}\text{O}$ : 0.06 ‰
AMS		Boulder (USA)	flasks	$\Delta^{14}\text{C}$ : 1.4–2.0 ‰

Title Page

Abstract

Introduction

Conclusions

References

Tables

Figures

◀

▶

◀

▶

Back

Close

Full Screen / Esc

Printer-friendly Version

Interactive Discussion





## Winter CO<sub>2</sub> emission in Paris

M. Lopez et al.

Title Page

Abstract

Introduction

Conclusions

References

Tables

Figures

◀

▶

◀

▶

Back

Close

Full Screen / Esc

Printer-friendly Version

Interactive Discussion



**Table 3.** CO<sub>2</sub>ff and CO<sub>2</sub>bio emissions with their respective contributions derived at the LHVP and at Jussieu.

Site	Nb of flasks	Date	CO <sub>2</sub> enhancement (ppm)		Respective repartition (%)	
			CO <sub>2</sub> ff	CO <sub>2</sub> bio	CO <sub>2</sub> ff	CO <sub>2</sub> bio
LHVP	8	4 Feb 2010	30.2	9.7	76	24
LHVP	3	5 Feb 2010	16.2	4.5	78	22
LHVP	3	9 Feb 2010	26.6	10.2	72	28
LHVP	3	10 Feb 2010	32.8	8.6	79	21
Jussieu	6	10 Feb 2010	25.1	6.9	78	22

## Winter CO<sub>2</sub> emission in Paris

M. Lopez et al.

**Table 4.**  $\frac{\text{CO}}{\text{CO}_2\text{ff}}$  ( $R_{\text{CO}}$ ) and  $\frac{\text{NO}_x}{\text{CO}_2\text{ff}}$  ( $R_{\text{NO}_x}$ ) ratios with their respective coefficients of determination ( $r^2$ ) for each sampled day and the corresponding values used for each regime.

Date	Wind regime	$R_{\text{CO}}$	$R_{\text{NO}_x}$
4 Feb 2010	oceanic	11.5 ( $r^2 = 0.75$ )	3.7 ( $r^2 = 0.89$ )
5 Feb 2010	oceanic	14.5 ( $r^2 = 0.90$ )	4.3 ( $r^2 = 0.96$ )
9 Feb 2010	continental	9.2 ( $r^2 = 0.97$ )	1.1 ( $r^2 = 0.92$ )
10 Feb 2010	continental	7.9 ( $r^2 = 1$ )	2.1 ( $r^2 = 0.91$ )
oceanic regime		13.0	4.0
continental regime		8.5	1.6
not clearly defined regime		10.8	2.8

Title Page

Abstract

Introduction

Conclusions

References

Tables

Figures

◀

▶

◀

▶

Back

Close

Full Screen / Esc

Printer-friendly Version

Interactive Discussion





## Winter CO<sub>2</sub> emission in Paris

M. Lopez et al.

**Table 6.** CO<sub>2</sub> contribution estimates by different inventories for the three main emission sectors. From the emission values, we computed the ratios  $R_{CO}$  and  $R_{NO_x}$  by sectors.

	Emission (%)			$R_{CO}$			$R_{NO_x}$		
	Road	Resid.	Ind.	Road	Resid.	Ind.	Road	Resid.	Ind.
CITEPA									
2005	31	24	24	11.1	16.5	18.1	5.9	1.1	2.0
2008	31	24	24	7.4	15.8	17.6	5.4	1.1	1.8
2010	31	25	23	5.3	14.5	17.5	4.8	1.1	1.7
EDGAR 4.2 France (2008)	32	24	27	4.4	15.1	0.8	3.5	1.4	2.2
EDGAR 4.2 Paris (2008)	73	12	9	5.4	1.0	0.9	4.3	2.0	4.0
IER Paris (2005)	36	45	15	12.8	19.8	0.4	4.3	1.2	3.6
AirParif Paris (Jan. 2008)	30	63	7				4.1	1.2	1.5

[Title Page](#)
[Abstract](#)
[Introduction](#)
[Conclusions](#)
[References](#)
[Tables](#)
[Figures](#)
[◀](#)
[▶](#)
[◀](#)
[▶](#)
[Back](#)
[Close](#)
[Full Screen / Esc](#)
[Printer-friendly Version](#)
[Interactive Discussion](#)


Winter CO<sub>2</sub> emission  
in Paris

M. Lopez et al.

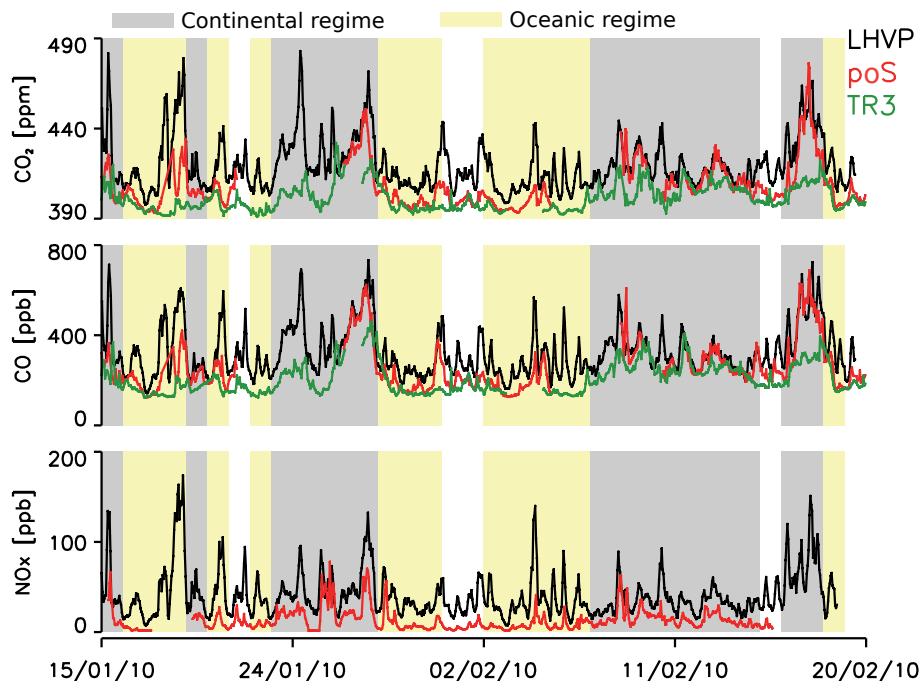


**Fig. 1.** The CO<sub>2</sub>, CO and NO<sub>x</sub> mole fractions at the LHVP, Plateau of Saclay (poS) and Trainou 180 m a.g.l. (TR3). Periods during which the air masses originate from the west are highlighted in yellow, and periods during which the air masses originate from the east are highlighted in grey. No colour is used for the days without a clear air mass origin.

[Title Page](#)[Abstract](#)[Introduction](#)[Conclusions](#)[References](#)[Tables](#)[Figures](#)[◀](#)[▶](#)[◀](#)[▶](#)[Back](#)[Close](#)[Full Screen / Esc](#)[Printer-friendly Version](#)[Interactive Discussion](#)

## Winter CO<sub>2</sub> emission in Paris

M. Lopez et al.

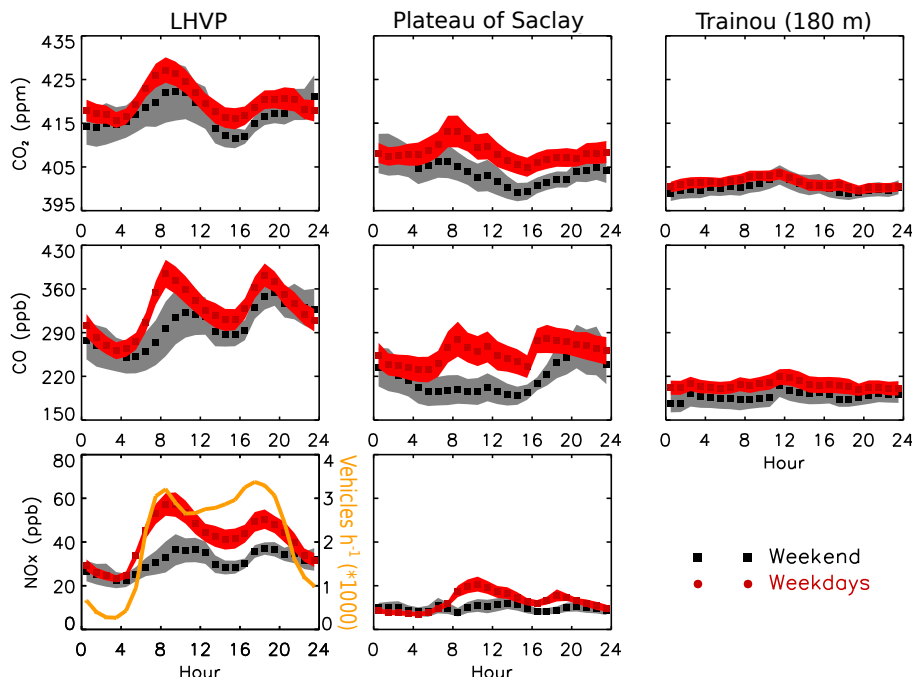


**Fig. 2.** Mean diurnal cycles of CO<sub>2</sub>, CO and NO<sub>x</sub> at the LHVP, Plateau of Saclay and Trainou sites for weekend and weekdays with the associated standard deviations. In the NO<sub>x</sub> plot for the LHVP, the mean diurnal cycle of vehicle flow during the weekdays for the year 2010 in Ile-de-France is added in orange (DIRIF).

Title Page

Abstract

Introduction

Conclusions

References

Tables

Figures

◀

▶

◀

▶

Back

Close

Full Screen / Esc

Printer-friendly Version

Interactive Discussion



Winter CO<sub>2</sub> emission  
in Paris

M. Lopez et al.

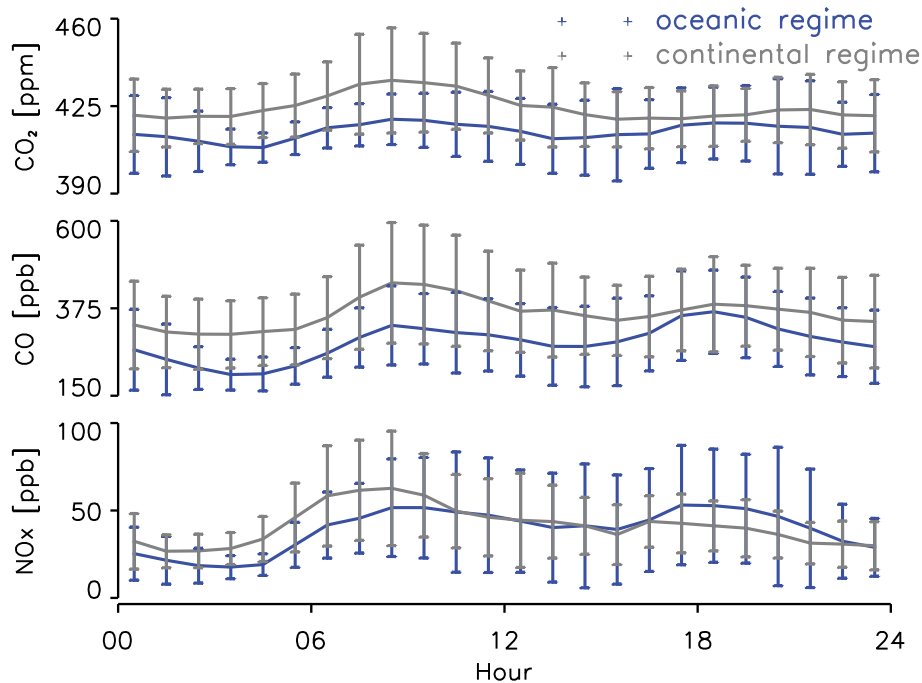


**Fig. 3.** The CO<sub>2</sub>, CO and NO<sub>x</sub> diurnal cycles at the LHVP as a function of the air mass regime. The grey curves correspond to the continental regime, whereas the blue curves correspond to the oceanic regime. The vertical lines represent the standard deviation of the mean.

[Title Page](#)[Abstract](#)[Introduction](#)[Conclusions](#)[References](#)[Tables](#)[Figures](#)[◀](#)[▶](#)[◀](#)[▶](#)[Back](#)[Close](#)[Full Screen / Esc](#)[Printer-friendly Version](#)[Interactive Discussion](#)

Winter CO<sub>2</sub> emission  
in Paris

M. Lopez et al.

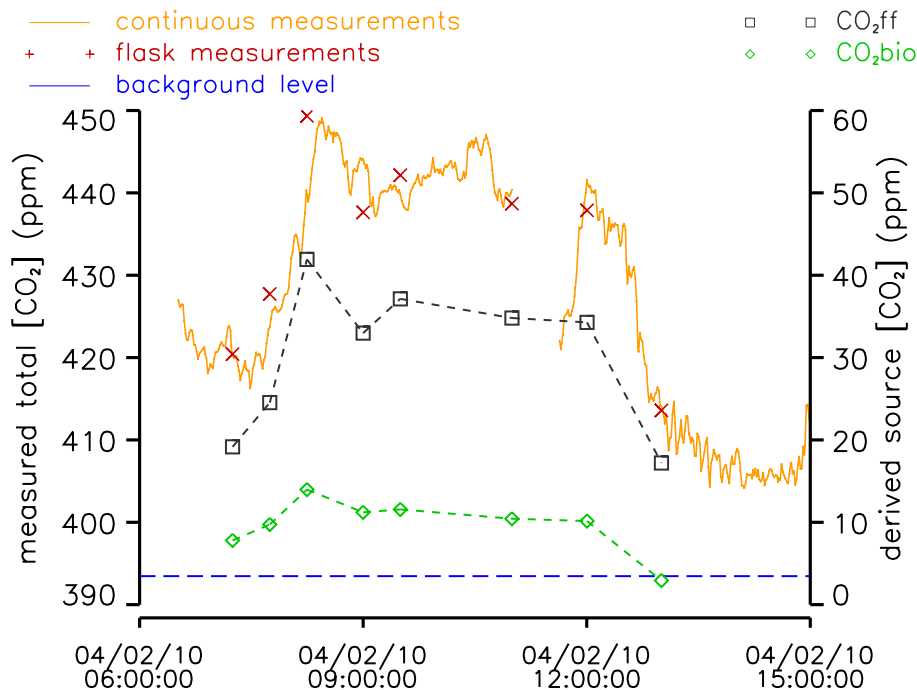


**Fig. 4.** A comparison between the continuous measurements for CO<sub>2</sub> (in orange) and the data obtained using flask sampling (red crosses) at the LHVP site are presented for 4 February 2010 on the left axis. We added the background level of CO<sub>2</sub> as measured at Mace Head (Ireland), which is represented by the blue dotted lines. The figures for CO<sub>2</sub>ff and CO<sub>2</sub>bio, as derived from flask sampling, are represented on the right axis by the black and green curves, respectively. The left and right axes have the same CO<sub>2</sub> amplitude.

[Title Page](#)
[Abstract](#)
[Introduction](#)
[Conclusions](#)
[References](#)
[Tables](#)
[Figures](#)
[◀](#)
[▶](#)
[◀](#)
[▶](#)
[Back](#)
[Close](#)
[Full Screen / Esc](#)
[Printer-friendly Version](#)
[Interactive Discussion](#)


Winter CO<sub>2</sub> emission  
in Paris

M. Lopez et al.

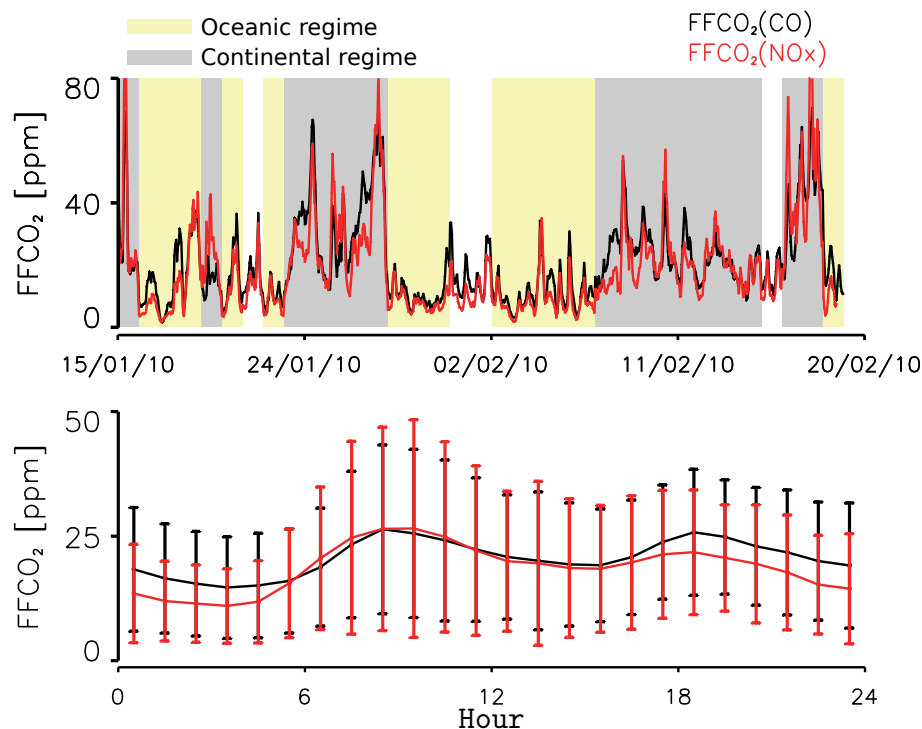


**Fig. 5.** Top: time series for FFCO<sub>2</sub> during the MEGAPOLI campaign calibrated using CO and NO<sub>x</sub> as proxies. Periods during which the air masses originate from the west are highlighted in yellow, and periods during which the air masses originate from the east are highlighted in grey. No colour is attributed on the days without a clear air mass origin (see Fig. 1). Bottom: mean diurnal cycles of FFCO<sub>2</sub>(CO) in black and FFCO<sub>2</sub>(NO<sub>x</sub>) in red at the LHVP station from 15 January 2010 to 20 February 2010.

[Title Page](#)[Abstract](#)[Introduction](#)[Conclusions](#)[References](#)[Tables](#)[Figures](#)[◀](#)[▶](#)[◀](#)[▶](#)[Back](#)[Close](#)[Full Screen / Esc](#)[Printer-friendly Version](#)[Interactive Discussion](#)